LAPPEENRANTA UNIVERSITY OF TECHNOLOGY Faculty of Technology Master's Degree Programme in Chemical Engineering

Matti Tähtinen

DEVELOPMENT OF CHEMICAL LOOPING COMBUSTION PROCESS

- Examiners: Professor Ilkka Turunen Professor Timo Hyppänen
- Supervisors: Antti Tourunen Jaakko Saastamoinen Toni Pikkarainen

ABSTRACT

Lappeenranta University of Technology Faculty of Technology Master's Degree Programme in Chemical Engineering

Matti Tähtinen

Development of chemical looping combustion process

Master's thesis

2010

99 pages, 35 figures, 10 tables.

Examiners: Professor Ilkka Turunen Professor Timo Hyppänen

Keywords: Chemical loop combustion, reactor design, oxygen carrier, reactor system

Chemical looping combustion (CLC) provides a promising technology to help cut carbon dioxide emissions. CLC is based on separated oxidation and reduction processes. Oxygen carrier, which is made from metal and supporting material, is in continuous recirculation between the air and fuel reactors. The CLC process does not require separation unit for carbon dioxide. The fuel reactor can produce an almost pure carbon dioxide feed which decrease costs of carbon capture and storage (CCS). The CLC method is one of the most promising ones for energy efficient carbon capture.

A large amount of literature was examined for this study and from it the most promising methods and designs were chosen. These methods and designs were combined as reactor system design which was then sized during the making of this thesis. Sizing was done with a mathematical model that was further improved during the study.

TIIVISTELMÄ

Lappeenrannan teknillinen yliopisto Teknillinen tiedekunta Kemiantekniikka

Matti Tähtinen

Kemikaalikierrollisen polttoprosessin kehittäminen

Diplomityö

2010

99 sivua, 35 kuvaa, 10 taulukkoa.

Tarkastajat:Professori Ilkka TurunenProfessori Timo Hyppänen

Hakusanat: Chemical loop combustion, reaktori suunnittelu, hapenkantaja, reaktori systeemi

Kemikaalikiertopoltto (CLC) on lupaava teknologia hiilidioksidipäästöjen leikkaamiseksi. CLC perustuu hapetus- ja pelkistysprosesseihin erillisissä leijupedeissä. Hapenkantaja on jatkuvassa kiertovirtauksessa ilma- ja polttoreaktoreiden välillä. CLC-prosessissa ei tarvita erillistä hiilidioksidin erotusyksikköä. Polttoreaktori kykenee tuottamaan lähes puhtaan hiilidioksidivirran hiilidioksidin sitomista ja talteenottoa varten (CCS). Tämän vuoksi CLC on energiatehokas tapa hiilen sitomiseksi.

Työ perustuu laajaan ja prosessin kannalta kattavaan lähdeaineistoon. Tästä lähdeaineistosta valittiin lupaavimmat reaktorisysteemin ominaisuudet eri reaktorilaitteistoista. Näitä ominaisuuksia yhdisteltiin reaktorilaitteiston suunnittelussa. Reaktorilaitteisto mitoitettiin kirjallisuuden ja matemaattisen mallin avulla. Matemaattista mallia kehitettiin työn aikana prosessiin paremmin soveltuvaksi.

PREFACE

This work was carried out in Jyväskylä at the Technical Research Center of Finland, VTT between June and December 2010. I am very flattered that I got to be a part of such a good team. This opportunity to show my knowledge has indeed been unique, and I can only hope that I was able to fit the bill.

I wish to thank my supervisors Antti Tourunen, Toni Pikkarainen and Jaakko Saastamoinen. Your generous help and our inspirational discussions have helped me tremendously to understand this technology and topic.

I would also like to thank Professor Ilkka Turunen and Professor Timo Hyppänen from the Lappeenranta University of Technology. I am very pleased for having had the opportunity of receiving interdisciplinary guidance from the university. I hope that this could be adopted as a guideline in the university with future theses operating on two or more fields of science.

I also wish to thank several mentors from the past few years who have greatly affected my studies and career. Esko Lahdenperä gave me a first peek into the world of simulation and modeling too fascinating to be ignored. I have also had the great privilege of working with Kalle Riihimäki who has taught me more than I could ever have imagined. Professor Andrzej Kraslawski from the university has opened my mind to creativity and has encouraged me to play with the mind. These people have pointed me to the direction where I am now and where I will be heading after this.

Finally, a big thank you to my mom and dad for the support and encouragement. Jenni, Hannes and Heikki, thank you for all the laughter and conversations during my life. Thank you to all my friends, fellow students and supporters.

Thank you Noora for your endless support and love during these years.

Ristiina, December 19th, 2010

Matti Tähtinen

CONTENTS

1	INT	RODUCTION	13
	1.1	Background	13
	1.2	Objectives and Restrictions	13
	1.3	-	13
•	CIU		4 =
2			15
	2.1	r · · · · · · · · · · · · · · · · · · ·	19
	2.2		20
		1	21
	a a		22
	2.3	50	24
			26
		1 1	26
	2.4		29 22
	2.4	6	33
		\mathcal{O}	34
			39
		1 8	41
			50
		8	50
	2.5	e	52
			52
		2.5.2 Validation	54
3	мо	DEL	56
-	3.1		56
		· · · ·	57
	3.2	1	58
	3.3		60
	3.4		66
	3.5		67
	0.0		0.
4	REA	ACTOR DESIGN	71
	4.1	Concept	72
	4.2	Reactor system	74
		4.2.1 Fuel reactor	74
		4.2.2 Air reactor	76
			79
		4.2.3 Cyclone	79 80
		4.2.3 Cyclone	
	4.3	4.2.3 Cyclone	80
	4.3 4.4	4.2.3 Cyclone 7 4.2.4 Particle locks 8 4.2.5 Loops 8 Measurement 8	80 81 81
		4.2.3 Cyclone 7 4.2.4 Particle locks 7 4.2.5 Loops 7 Measurement 7 Conditions 7	80 81
	4.4	4.2.3Cyclone74.2.4Particle locks84.2.5Loops8Measurement8Conditions8Possible problems8	80 81 81 83 84
	4.4	4.2.3Cyclone74.2.4Particle locks74.2.5Loops7Measurement7Conditions7Possible problems74.5.1Gas leakage between reactors7	80 81 83 84 84
	4.4	4.2.3Cyclone74.2.4Particle locks84.2.5Loops8Measurement8Conditions8Possible problems84.5.1Gas leakage between reactors84.5.2Emissions8	80 81 81 83

	4.7	4.6.1 Design	•															
5		ULTS A Future v		 	-			•		•		•			•		•	90 91
Rŀ	EFER	ENCES																93

ABBREVIATIONS

ASU	Air separation unit
CCS	Carbon capture and storage
CFB	Circulating fluidized bed
CFD	Computational fluid dynamics
CLC	Chemical looping combustion
DCFB	Dual circulating fluidized bed
EFR	Entrained flow reactor
GPGPU	General-purpose computing on graphics pro-
	cessing units

SYMBOLS

ArArchimedes number- c Concentrationmol/dm³ c Specific heat capacityJ kg ⁻¹ K ⁻¹ d Diameterm f Radiation coefficient- f Stoichiometric mass ratio- Fr Froude number- g Gravitym²s ⁻¹ H Reaction heat J/kg h Heat transfer coefficientkg m²s ⁻¹ k Reaction rate coefficientkg m²s ⁻¹ k Reaction rate coefficientkg m²s ⁻¹ k Reaction rate coefficientkg m²s ⁻¹ k Neaction rate coefficientkg s²s ⁻¹ k Neaction rate coefficientkg s²s ⁻¹ k NuMolar massg/mol m Masskgn m Mass flow ratekg s²s ⁻¹ Nu Nusselt number- Pr Prandtl number- p PressurePa R True oxygen transport capacity of material- Re Reynolds number S Surface aream² S''' Particle surface area/volume of reactorm ⁻¹ T TemperatureK t Times V Volumem³ u, v, w Velocitym/s X Conversion- Y Mass fraction-	A	Area	m^2
c Specific heat capacity $J kg^{-1} K^{-1}$ d Diameterm F Radiation coefficient- f Stoichiometric mass ratio- Fr Froude number- g Gravity $m^{2}s^{-1}$ H Reaction heat J/kg h Heat transfer coefficient $kg m^{-2}s^{-1}$ k Reaction rate coefficient $kg m^{-2}s^{-1}$ L Lengthm M Molar mass g/mol m Mass $kg s^{-1}$ Nu Nusselt number- Pr Prandtl number- p PressurePa R True oxygen transport capacity of material- Re Reynolds number- S Surface area m^{2} S''' Particle surface area/volume of reactor m^{-1} T Times V Volume m^{3} u, v, w Velocity m/s	Ar	Archimedes number	-
dDiameterm F Radiation coefficient- f Stoichiometric mass ratio- Fr Froude number- g Gravity $m^{2}s^{-1}$ H Reaction heat J/kg h Heat transfer coefficient $kg m^{-2}s^{-1}$ k Reaction rate coefficient $kg m^{-2}s^{-1}$ L Lengthm M Molar mass g/mol m Massflow rate $kg s^{n-1}$ NuNusselt number Pr Prandtl number- Pr PressurePa R True oxygen transport capacity of material- Re Reynolds number- S Surface area m^{2} S''' Particle surface area/volume of reactor m^{-1} T Times V Volume m^{3} u, v, w Velocity m/s X Conversion-	С	Concentration	mol/dm ³
dDiameterm F Radiation coefficient- f Stoichiometric mass ratio- Fr Froude number- g Gravity $m^{2}s^{-1}$ H Reaction heat J/kg h Heat transfer coefficient $kg m^{-2}s^{-1}$ k Reaction rate coefficient $kg m^{-2}s^{-1}$ L Lengthm M Molar mass g/mol m Massflow rate $kg s^{n-1}$ NuNusselt number Pr Prandtl number- Pr PressurePa R True oxygen transport capacity of material- Re Reynolds number- S Surface area m^{2} S''' Particle surface area/volume of reactor m^{-1} T Times V Volume m^{3} u, v, w Velocity m/s X Conversion-	С	Specific heat capacity	$J kg^{-1}K^{-1}$
f Stoichiometric mass ratio- Fr Froude number- g Gravity m^2s^{-1} H Reaction heat J/kg h Heat transfer coefficient $kg m^{-2}s^{-1}$ k Reaction rate coefficient $kg m^{-2}s^{-1}$ L Lengthm M Molar mass g/mol m Mass kg \dot{m} Mass flow rate $kg s^{-1}$ Nu Nusselt number- Pr Prandtl number- p PressurePa R True oxygen transport capacity of material- R_0 Oxygen transport capacity of metal oxide- S Surface area m^2 S''' Particle surface area/volume of reactor m^{-1} T Times V Volume m^3 u, v, w Velocity m/s X Conversion-	d		•
Fr Froude number-gGravity $m^2 s^{-1}$ HReaction heat J/kg hHeat transfer coefficient $kg m^{-2} s^{-1}$ kReaction rate coefficient $kg m^{-2} s^{-1}$ LLengthmMMolar mass g/mol mMass kg \dot{m} Mass flow rate $kg s^{-1}$ NuNusselt number-PrPrandtl number-pPressurePaRTrue oxygen transport capacity of material- R_0 Oxygen transport capacity of metal oxide-SSurface area m^2 S'''Particle surface area/volume of reactor m^{-1} TTemperatureKtTimesVVolume m^3 u, v, w Velocity m/s XConversion-	F	Radiation coefficient	-
gGravity $m^{2}s^{-1}$ HReaction heat J/kg hHeat transfer coefficient $kg m^{-2}s^{-1}$ kReaction rate coefficient $kg m^{-2}s^{-1}$ LLengthmMMolar mass g/mol mMasskg \dot{m} Mass flow rate $kg s^{-1}$ NuNusselt number-PrPrandtl number-pPressurePaRTrue oxygen transport capacity of material-ReReynolds number-SSurface aream^2S'''Particle surface area/volume of reactorm^{-1}TTemperatureKtTimesVVolumem ³ u, v, wVelocitym/sXConversion-	f	Stoichiometric mass ratio	-
H Reaction heat J/kg h Heat transfer coefficient $kg m^{-2}s^{-1}$ k Reaction rate coefficient $kg m^{-2}s^{-1}$ L Lengthm M Molar mass g/mol m Mass kg m Massflow rate kg m^{-1} Nu Nusselt number Pr Prandtl number p Pressure Pa R R True oxygen transport capacity of material Re Reynolds number S Surface area S'''' Particle surface area/volume of reactor T Temperature K Time V Volume w Velocity X Conversion	Fr	Froude number	-
HReaction heatJ/kghHeat transfer coefficientkg m^{-2}s^{-1}kReaction rate coefficientkg m^{-2}s^{-1}LLengthmMMolar massg/molmMasskg \dot{m} Mass flow ratekg s^{-1}NuNusselt number-PrPrandtl number-PPressurePaRTrue oxygen transport capacity of material-ReReynolds number-SSurface aream^2S''''Particle surface area/volume of reactorm^{-1}TTemperatureKtTimesVVolumem ³ u, v, wVelocitym/sXConversion-	g	Gravity	$m^2 s^{-1}$
hHeat transfer coefficientkg m^{-2}s^{-1}kReaction rate coefficientkg m^{-2}s^{-1}LLengthmMMolar massg/molmMasskg \dot{m} Mass flow ratekg s^{-1}NuNusselt number-PrPrandtl number-pPressurePaRTrue oxygen transport capacity of material-ReReynolds number-SSurface aream^2S''''Particle surface area/volume of reactorm^{-1}TTemperatureKtTimesVVolumem ³ u, v, wVelocitym/sXConversion-		Reaction heat	J/kg
kReaction rate coefficientkg m^{-2}s^{-1}LLengthmMMolar massg/molmMasskg m Mass flow ratekg s^{-1}NuNusselt number-PrPrandtl number-pPressurePaRTrue oxygen transport capacity of material- R_0 Oxygen transport capacity of metal oxide-SSurface aream^2S'''Particle surface area/volume of reactorm^{-1}TTemperatureKtTimesVVolumem ³ u, v, wVelocitym/sXConversion-	h	Heat transfer coefficient	
M Molar massg/mol m Masskg \dot{m} Mass flow ratekg s ⁻¹ Nu Nusselt number- Pr Prandtl number- p PressurePa R True oxygen transport capacity of material- R_0 Oxygen transport capacity of metal oxide- Re Reynolds number- S Surface area m^2 S''' Particle surface area/volume of reactor m^{-1} T TemperatureK t Times V Volume m^3 u, v, w Velocity m/s X Conversion-	k	Reaction rate coefficient	
m Masskg \dot{m} Mass flow ratekg s ⁻¹ Nu Nusselt number- Pr Prandtl number- Pr Prandtl numberPa R True oxygen transport capacity of material- R_0 Oxygen transport capacity of metal oxide- Re Reynolds number- S Surface area m^2 S''' Particle surface area/volume of reactor m^{-1} T TemperatureK t Times V Volume m^3 u, v, w Velocitym/s X Conversion-	L	Length	m
\dot{m} Mass flow ratekg s^{-1} Nu Nusselt number- Pr Prandtl number- p PressurePa R True oxygen transport capacity of material- R_0 Oxygen transport capacity of metal oxide- Re Reynolds number- S Surface area m^2 S''' Particle surface area/volume of reactor m^{-1} T TemperatureK t Times V Volume m^3 u, v, w Velocity m/s X Conversion-	Μ	Molar mass	g/mol
Nu Nusselt number- Pr Prandtl number- p PressurePa R True oxygen transport capacity of material- R_0 Oxygen transport capacity of metal oxide- Re Reynolds number- S Surface area m^2 S''' Particle surface area/volume of reactor m^{-1} T TemperatureK t Times V Volume m^3 u, v, w Velocitym/s X Conversion-	т	Mass	kg
Pr Prandtl number- p PressurePa R True oxygen transport capacity of material- R_0 Oxygen transport capacity of metal oxide- R_0 Oxygen transport capacity of metal oxide- Re Reynolds number- S Surface area m^2 S''' Particle surface area/volume of reactor m^{-1} T TemperatureK t Times V Volume m^3 u, v, w Velocity m/s X Conversion-	ṁ	Mass flow rate	kg s $^{-1}$
p PressurePa R True oxygen transport capacity of material- R_0 Oxygen transport capacity of metal oxide- Re Reynolds number- S Surface area m^2 S''' Particle surface area/volume of reactor m^{-1} T TemperatureK t Times V Volume m^3 u, v, w Velocity m/s X Conversion-	Nu	Nusselt number	-
RTrue oxygen transport capacity of material- R_0 Oxygen transport capacity of metal oxide- Re Reynolds number-SSurface area m^2 S'''Particle surface area/volume of reactor m^{-1} TTemperatureKtTimesVVolume m^3 u, v, wVelocitym/sXConversion-	Pr	Prandtl number	-
R_0 Oxygen transport capacity of metal oxide- Re Reynolds number- S Surface area m^2 S''' Particle surface area/volume of reactor m^{-1} T TemperatureK t Times V Volume m^3 u, v, w Velocity m/s X Conversion-	р	Pressure	Pa
Re Reynolds number- S Surface area m^2 S''' Particle surface area/volume of reactor m^{-1} T TemperatureK t Times V Volume m^3 u, v, w Velocitym/s X Conversion-	R	True oxygen transport capacity of material	-
SSurface area m^2 S'''Particle surface area/volume of reactor m^{-1} TTemperatureKtTimesVVolume m^3 u, v, wVelocitym/sXConversion-	R_0	Oxygen transport capacity of metal oxide	-
S''' Particle surface area/volume of reactor m^{-1} T TemperatureK t Times V Volume m^3 u, v, w Velocitym/s X Conversion-	Re	Reynolds number	-
T TemperatureK t Times V Volume m^3 u, v, w Velocitym/s X Conversion-		Surface area	m^2
tTimestTimesVVolumem³u, v, wVelocitym/sXConversion-	<i>S'''</i>	Particle surface area/volume of reactor	m^{-1}
V Volume m^3 u, v, w Velocity m/s X Conversion-	Т	Temperature	Κ
u, v, wVelocitym/sXConversion-	t	Time	S
X Conversion -	V	Volume	m^3
	и, v, w	Velocity	m/s
Y Mass fraction -			-
	Y	Mass fraction	-

Greek letters

β	$\beta = \rho_{min} / \rho_{max}$	-
γ	Gas yield	-
ε	Voidage, porosity, emissivity	-
λ	Air ratio	-
μ	Dynamic viscosity	Pa s
ρ	Density	$\mathrm{kg}~\mathrm{m}^{-3}$
σ	Stefan-Bolzmann's constant	$5.67 \text{x} 10^{-8} \text{ W K}^{-4}$
au	Time of complete conversion of fresh particle	-
Φ'	Heat loss/length of reactor	$\mathrm{W}~\mathrm{m}^{-1}$
ϕ	Roundness	-

Subscripts

0	initial, inlet
b	reactor bed
bed	reactor bed
С	conversion
D	drag
8	gas
i	species $(O_2, CH_4, H_2 \text{ or } CO_2)$
max	maximum
mf	minimum fluidization
min	minimum
ox	oxidized
р	particle
r	radiation
reac	reactor
red	reduced
s, sol	solid
t	terminal, thermal
th	thermal
W	wall

LIST OF FIGURES

1	Basic concept of CLC-process and oxygen carrier circulation	15
2	Pressure drop versus gas velocity for a bed of uniformly sized sand particles	21
2	1	21
3	Effect of porosity on the maximum temperature increase inside of	0.1
4	the particle	31
4	Effect of particle size on the solid conversion and the maximum	~~
_	temperature	33
5	Reactor design presented by Lyngfelt et al	35
6	Reactor design with recycle loops	36
7	Reactor design for oxygen carrier tests	39
8	Schematic description of the improved reactor for oxygen carrier tests by Rydén et al.	40
9	Schematic description of 500W reactor by Adánez et al	42
10	Schematic diagram of CFB reactor for CLC by Son & Kim	43
11	The basic relations between carrier reactivity and design input data	
	by Lyngfelt et al.	44
12	Design procedure of a chemical-looping combustor by Kronberger	• •
12	et al	45
13	Schematic diagram of a 50kWth chemical-looping combustion sys-	10
15	tem by Ryu et al.	46
14	Typical structure of fluid dynamic description of fast fluidized bed	10
11	reactors by Kolbitsch, Pröll & Hofbauer	47
15	DCFB reactor system set-up. Both AR and FR are designed as cir-	• • •
10	culating fluidized beds by Kolbitsch et al.	48
16	Schematics of reactor by Alstom Power Inc.	49
17	Schematic of conventional two interconnected circulating fluidized	
17	bed system.	50
18	Schematic of a two bubbling bed interconnected circulating flu-	00
10	idized bed system by Ryu et al.	51
19	Main equations and variables at model	59
20	Model structure and simulation phases	62
21	Velocities at air reactor	68
22	Velocities at fuel reactor	68
23	Gas mass fractions at fuel reactor	69
24	Conversion of CH4 at fuel reactor	69
25	Conversion state of oxygen carrier at fuel reactor	70
26	Design procedure with fixed properties and initial conditions	72
27	Interrelationship of variables during sizing	73
28	Conversion of fuel at fuel reactor	77
29	Parameter run at fuel reactor	78
30	Conversion of Cu-based oxygen carrier	79
31	Cyclone shape and dimensions	80
32	Schematic diagram of loop-seal	82
33	Loop-seal of a large commercial CFB boiler with a twin recycle	
	chamber	83
		-

34	Locations for measurements at reactor design	84
35	Summary of design	89

LIST OF TABLES

1	Reactions of the metal oxides used in CLC	27
2	Effect of particle size and sintering temperature on particle properties	28
3	Contradiction between crushing strength and porosity	32
4	Oxygen carrier physical properties	60
5	Oxygen carrier reactivity properties	61
6	Physical properties of reactors	74
7	Design properties of fuel reactor	75
8	Design properties of air reactor	78
9	Cyclone dimensions	81
10	Main reactor system dimensions and area of operation	88

1 INTRODUCTION

1.1 Background

 CO_2 emissions have been increasing due to human actions because fossil fuels, which cause a large portion of the CO_2 emissions, are still an important part of the world's energy resources. In order to decrease the effects of human actions on the environment new technologies have to be developed. This challenges the science society to improve the already existing technology as well as to create new innovations.

One of the developments is carbon capture and storage, CCS. Carbon capture can be done in multiple ways; one of the most promising ways is the oxy-fuel combustion by chemical loop combustion, CLC. Theory of CLC (Richter & Knoche 1983) was first introduced in 1983. Ever since it has gave one way to decrease CO2 emission significantly. Development does not come easy even in this field of science. Over two decades later, first prototypes were introduced in literature and we can now see the dawn of new technology.

1.2 Objectives and Restrictions

The objective of this thesis is to develop chemical looping combustion research by improving the computational model and by designing a lab-size reactor for chemical loop combustion. Computational models of air and fuel reactors will be combined as one. The reactor design will be done with computational models and measurement data. This thesis does not include the building of the reactor or the testing of it.

1.3 Structure of the Thesis

This report is organized as follows: In Section 2., process principles, basic phenomenas and the concept of fluidized bed are briefly explained. The section also includes discussion on oxygen carriers, different kinds of reactor designs and a short comment about modeling. In Section 3., the mathematical model used in the simulation is explained. The limitations and structure of the model are introduced in this section.

The chosen reaction design is presented in Section 4. This section offers information on what kind of a concept is chosen and what kind of equipments will be used in the reactor system. Main equipments are viewed separately.

Section 5. combines the results of the thesis. Also future work on technology and research connected to this thesis are discussed.

2 CHEMICAL-LOOPING COMBUSTION

Chemical-looping combustion (CLC) is based on two reactions which take place at two different sections and in turns. These reactions are oxidation and reduction reactions. Usually the sections are called the air reactor and the fuel reactor. Oxygen carrier transfers oxygen and heat from one section to another.

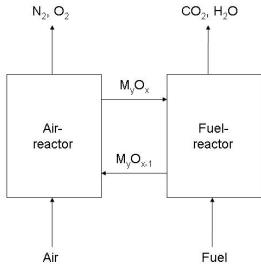


Figure 1. Basic concept of CLC-process and oxygen carrier circulation (Johansson 2007)

Basic concept of CLC is illustrated at Fig. 1. Oxygen carrier circulates between an air and a fuel reactor. In the air reactor, the oxygen carrier is oxidized, which is always an exothermic reaction. The air reactor has inlet from air and outlet of depressed air. The outlet contains nitrogen and a decreased amount of oxygen. The outlet is also hotter than the inlet because of the exothermic reaction. These gases can be released without harm to nature. The oxygen carrier flow is taken to fuel reactor where a reduction reaction takes place. The reduction reaction can be either exothermic or endothermic depending on the oxygen carrier. Fuel is the inlet for fuel reaction and the outlet contains mainly CO_2 and small amounts of H_2O . (Hossain & de Lasa 2008)

Reactions taking place in the process are quite simple because the process is based on oxidation and reduction reactions. These two reactions and their combination can be seen at Eq. 1., 2. and 3. The reactions are gas-solid reactions where fuel and air refer to gas and particles refer to solid phase. The reactions take place on the surface of the particles. Reaction at air reactor:

$$(2n+m)M_yO_{x-1} + (n+\frac{1}{2}m)O_2 \Rightarrow (2n+m)M_yO_x$$
 (1)

Reaction at fuel reactor:

$$(2n+m)M_yO_x + C_nH_{2m} \Rightarrow (2n+m)M_yO_{x-1} + mH_2O + nCO_2$$
 (2)

Net reaction:

$$C_n H_{2m} + (n + \frac{1}{2}m)O_2 \Rightarrow mH_2O + nCO_2$$
(3)

As mentioned earlier, reaction 1. is exothermic and reaction 2. can be either exothermic or endothermic depending on the metal oxide. The amount of escaped energy depends on the metal oxide and fuel that was used. Difference to normal combustion is that nitrogen in air is not diluted to combustion gases. Therefore, separation unit between CO_2 and nitrogen from the fuel reactor outlet is not needed.

Only the steam that has been diluted to the stream needs to be separated. This can easily be condensed from the stream. No other processing is needed for high concentrated CO_2 stream. In literature (Johansson 2007), approximate temperature in the process has been evaluated to 800–1200 °C and the process can be at atmospheric pressure or pressurized.

Oxygen transport capacity or oxygen ratio, R_O , defines how much oxygen the carrier can transport to process. This ratio is essential for correct sizing. R_O is defined at Eq. 4.

$$R_O = \frac{M_{ox} - M_{red}}{M_{ox}} \tag{4}$$

where M_{ox} is the molar mass of fully oxidized oxygen carrier M_{red} is the molar mass of fully reduced oxygen carrier.

If the temperature rises over 1600° C in the air reactor, NO_x can be formed. As we can see, the temperatures are not high enough for NO_x to form. Surveys have not found any signs of NO_x formation at the CLC-process. Temperature in the fuel reactor is lower that in the air reactor. If the fuel contains parent substances, normal emissions of combustion take place. It is possible that NO_x can be formed, but the fuel reactor conditions are not favorable. This has not yet been experimentally verified. From the point of view of developing nature friendly technologies , this aspect of the CLC process is both interesting and competitive. (Ishida & Jin 1996).

Oxidation reaction is usually more rapid than reduction reaction, but this depends on the oxygen carrier. When the concentration of the reacting gas lowers, the conversion decreases. This leads to a state where conversion of fuel is not fully obtained.

A possible side reaction in the fuel reactor is carbon formation. Two main ways for carbon formation are the Boudouard reaction, Eq. 5. and pyrolysis, Eq. 6. Coke formation is an unwanted phenomenon which may lead to carbon leak. Carbon can attach to the particle surface and be oxidized when the particle is introduced to the air reactor, seen here at Eq. 7. (Hossain & de Lasa 2008). This would decrease carbon capture efficiency.

$$2CO \Leftrightarrow C + CO_2 \tag{5}$$

Boudouard reaction is exothermic and more easily takes place at lower temperatures. Pyrolysis reaction is endothermic and is favored at high temperatures. Kinetically, both Ni and Fe can act as a catalyst on Boudouard and pyrolysis reactions (Hossain & de Lasa 2008).

$$C_n O_{2n+2} \Leftrightarrow nC + (n+1)H_2 \tag{6}$$

$$C + O_2 \Rightarrow CO_2 \tag{7}$$

Other reactions may also happen in the fuel reactor. Especially Ni -based oxygen carriers have catalytic properties that may lower the needed activation energy for Eq. 8. and 9. Small amounts of Ni in the oxygen carrier particle or a mixture of oxygen carriers enable these reactions and increase methane conversion. (Johansson 2007)

Methane pyrolysis reaction:

$$CH4 + H_2O \Leftrightarrow CO + 3H_2 \tag{8}$$

Gas-Water shift reaction is not as harmful as carbon formation reactions. Water as a reaction product or the steam from particle locks reacts with carbon monoxide. Reaction equation is presented at Eq. 9.

Water shift reaction:

$$CO + H_2O \Leftrightarrow CO_2 + H_2$$
 (9)

Energy net reaction:

$$\Delta H_c = \Delta H_{red} + \Delta H_{oxd} < 0 \tag{10}$$

Total net heat of these two reactions is the same as if the combustion had been done with air. When compared to rival combustion technologies, there are no thermal energy advantages in the CLC-process. However, one of its main advantages is an easily obtained CO_2 stream. Also the output streams into nature do not need any purification. (Hossain & de Lasa 2008)

When different combustion processes are compared with carbon capture and storage (CCS), some additional energy advantages can be found. Studies illustrate that conventional systems with carbon capture are less thermal efficient. When it comes to capital costs, the advantage of CLC-processes is that air separation unit (ASU) is not needed for CO_2 separation (Johansson 2007). Another way of producing a pure CO_2 stream after combustion is by oxy-fuel combustion. This needs a sustained oxygen flow made with an oxygen-plant. Oxygen-plant, however, consumes a lot of energy. Capital and operational costs become higher than with energy produced with CLC -process.

When it comes to reliable calculations, the lack of long term survey produces a problem. There are no data based on which preliminary assumptions could be proven. Because of these circumstances, CLC technology has not yet revealed its full potential.

In literature, fuel has usually been treated as natural gas or syngas. Another possibility is to use solid fuels. This is a field which does not have very many references to it in literature. However, a few surveys (Leion et al. 2009, 2007, 2008) have referred to CLC and solid fuels. What is looked for in the surveys is a cheap oxygen carrier, because it can be assumed that friction forces increase when fuel is solid. Oxygen carrier will probably wear faster with solid fuel. Cao et al. (2006) have investigated how solid fuels, especially biomass and solid waste, are suitable for CLC. Survey concludes that solid fuels which have the characteristics of volatile matter are suitable for fuel. One example is low-density polyethylene. The beauty of volatile solid waste is that CLC-process that uses it as raw material decreases CO_2 emissions. The carbon of solid waste would otherwise be released into the atmosphere. Waste is also cheap or perhaps even entirely free raw material, which is important if we wish to increase the profitability of the process.

2.1 Experimental research

Research aimed at CLC is mainly quantitative. To be more accurate, it has been primary research. Characteristic for this primary research is that its purpose is to receive initial data about the research subject. The problem with this kind of research is the lack of more comprehensive results as it provides only a hint of what should be inspected more deeply. Primary study is also quite expensive and it has to be accurate because it will serve as the basis for later studies.

Major contributors for oxygen carrier research have been CSIC in Zaragoza, Spain, Chalmers University of Technology in Gothenburg, Sweden, Tokyo Institute of Technology in Japan and Korea Institute of Energy Research (Johansson 2007). This can be seen as primary research.

Not all primary studies are fully comparable because the research has not been done in the same reactor construction or at the same facilities. The conclusions of the studies are more comparable.

Primary research can be seen as being initiatory CLC research. Hundreds of oxygen carriers have already been tested. Based on these tests, we can make further hypothesis and test them. In order to receive funding, it is important that there already is something concrete to show and that there is a well specified hypothesis to prove. Extensive and well executed primary research hopefully increases the funding of secondary research.

Secondary research makes a hypothesis based on the data received from the primary research and combines earlier surveys for larger synthesis. There are a couple of more extensive reviews from the field of CLC which are comprehensive (Fang et al.

2009, Hossain & de Lasa 2008, Lyngfelt et al. 2008). These reviews combine earlier studies as one guideline of research and create a good cross-section profile of the studies.

An example of secondary research is the approved hypothesis where additives at oxygen carrier enable better properties than pure oxides (Jerndal et al. 2009). This kind of research provides examples and new conclusions of how oxygen carrier works and how the process can be predicted.

Experimental research generally consists of measurements and tests. Usually the experiments have compared oxygen carriers and their properties. Surveys which compare different kinds of process designs are not to be found in literature. Reactors are expensive to construct and comparison of alternative reactor designs is needed for comprehensive surveys.

Oxygen carriers are evaluated from how well selections are suitable for the wanted process type. The aim of experimental research is to find and validate knowledge and models to real world conditions. The tools for the experiments differ, but research on reactor design and oxygen carriers are connected.

2.2 Fluidized bed

Chemical-looping combustion has great similarities with common fluidized bed combustion. Fluidized bed combustion is divided into three groups, which are bubbling, turbulent and circulating bed. Solids stay at bed at bubbling bed combustion. At turbulent bed particle flow is turbulent. Solids are dragged by gas flow to circulation at circulating bed. The hydrodynamics of an air reactor with a riser is close to the circulating bed and some fuel reactor designs have similarities with the bubbling bed.

Depending on gas velocity, bed construction can be divided into four sections: fixed bed, bubbling bed, turbulent bed and circulating bed. When gas velocity increases, solid content at the bottom decreases and increases at the top of the boiler. Circulation changes to pneumatic transport if velocity increases high enough. (Raiko et al. 2002)

2.2.1 Pressure drop

Pressure drops happen at process. Pressure drop is based on different phenomena depending on the subprocess. Pressure drop changes depending on gas velocity. Pressure drop compared to velocity can be seen at Fig. 2.

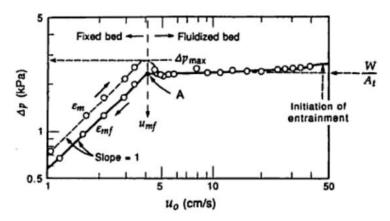


Figure 2. Pressure drop versus gas velocity for a bed of uniformly sized sand particles (Kunii & Levenspiel 1977)

The figure shows a small leap at pressure drop when gas velocity is at minimum fluidizing velocity, u_{mf} . This leap separates fixed and fluidized beds. After this comes the initiation of entrainment velocity when particles are entrained to gas flow.

Initiation of entrainment level at Fig. 2. means the level where particles start to entrain to the gas flow. This level depends on the size distribution of the particles. Particle size defines the gas velocity needed.

Pressure drop at fluidized bed can be calculated from Eq. 11.

$$\Delta p = \frac{m_{bed}g}{A_{reactor}} \tag{11}$$

 m_{bed} is connected to height of bed, h_{bed} , via Eq. 12.

$$m_{bed} = h_{bed} \rho_p (1 - \epsilon) A_{reac} \tag{12}$$

2.2.2 Flows at system

Gas flows are introduced to the system at higher pressure. Pressure difference forms the driving force for gaseous fluids. Gas flows are the main drag force in solid circulation. The second important drag force is gravitation. Level of significance of the driving force depends on the reactor.

The gas flow has to exceed the effect of gravitation for it to enable solid circulation at reactor if a circulated fluidized bed is wanted. The case of the bubbling bed takes place if gravitation forces exceed the gas flow and solids drop at the bottom of the reactor. Minimum fluidizing velocity has to be exceeded in order for these phenomena to occur.

Simplified equation for minimum fluidized conditions is presented at Eq. 13.

$$\frac{\Delta p}{L_{mf}} = (1 - \epsilon_{mf})(\rho_s - \rho_g)\frac{g}{g_c}$$
(13)

where	Δp	is the pressure drop across bed
	L_{mf}	is the bed height at minimum fluidizing condi-
		tions
	ϵ_{mf}	is the void fraction at minimum fluidizing con-
		ditions
	$ ho_s$	is the density of solids
	$ ho_g$	is the density of gas
	g	is the acceleration of gravity
	g_c	is the conversion factor.

Minimum fluidization velocity is the velocity needed to provide the flow for particle fluidization. When the minimum fluidization velocity is exceeded, the bed starts to fluidize. If the velocity is increased enough, the particles are entrained with flowing gas. Minimum fluidization velocity (Kunii & Levenspiel 1977) is presented at Eq. 14.

$$\frac{1.75}{\phi_s \varepsilon_{mf}^3} \left(\frac{d_p u_{mf} \rho g}{\mu}\right)^2 + \frac{150(1 - \varepsilon_{mf})}{\phi_s^2 \varepsilon_{mf}^3} \left(\frac{d_p u_{mf} \rho g}{\mu}\right) = \frac{d_p^3 \rho_g (\rho_s - \rho_g) g}{\mu^2}$$
(14)

where	ϕ_s	is the roundness of particle
	ε_{mf}	is the voidage at minimum fluidizing conditions
	u_{mf}	is the minimum fluidization velocity
	g	is the standard gravity
	μ	is the dynamic viscosity of gas

which can be simplified if Eq. 16. and 17. are combined to Eq. 14.

$$\frac{1.75}{\phi_s \varepsilon_{mf}^3} R e_{p,mf}^2 + \frac{150(1 - \varepsilon_{mf})}{\phi_s^2 \varepsilon_{mf}^3} R e_{p,mf} = Ar$$
(15)

$$Re = \frac{d_p u_{mf} \rho g}{\mu} \tag{16}$$

$$Ar = \frac{d_p^3 \rho_g (\rho_s - \rho_g)g}{\mu^2} \tag{17}$$

Minimum fluidization velocity has to be solved iteratively from Eq. 14. Values for voidage at minimum fluidizing conditions, ε_{mf} , can be estimated from literature or measured experimentally. When particle size decreases, voidage increases.

Terminal velocity, u_t , is velocity when bed fluidization reaches the point where particles are entrained to gas flow. Terminal velocity, u_t , can be calculated from Eq. 18.,

$$u_t = \left(\frac{4}{3}d_p \frac{(s-1)}{C_D}g\right)^{\frac{1}{2}}$$
(18)

where

$$s = \frac{\rho_s}{\rho_g} \tag{19}$$

At the equation, drag coefficient, C_D , can be determined experimentally or from analytical expression. Drag coefficient depends on particle shape, but usually simplification for spherical shape is made. Analytical expression has to be chosen by using Reynolds number, Re_p . When Reynolds number is 2000...200000, C_D can be simplified to 0,44 (Raiko et al. 2002). It is essential that the minimum fluidizing and terminal velocities are known and that the velocities are controllable. Specific hydrodynamic patterns at reactor depend on material properties and reactor structure.

2.3 Oxygen carriers

The oxygen carrier is the most essential component of the CLC process. It transfers heat and oxygen at the process. Both are needed for a robust process. Many design issues depend on the properties of the oxygen carrier. An important property of the oxygen carrier is the oxygen carrying capacity. Circulation rate is highly dependent on this character. Therefore, it is important to have an oxygen carrier that has good reactivity at both oxidation and reduction reaction. Also, it is important that the oxygen carrier burns fuel fully.

Hossain & de Lasa (2008) have listed six other important characteristics of a good oxygen carrier. According to them, a good oxygen carrier should:

- 1. be chemically stable under repeated oxidation/reduction cycles at high temperature,
- 2. be fluidizable,
- 3. be resistant to agglomeration,
- 4. *be mechanical resistant to the friction stress associated with high circulation of particles,*
- 5. be environmentally safe and
- 6. be economically feasible.

In literature, oxygen carrier research has focused on the development of a suitable oxygen carrier. Oxygen carriers differ between each other. Major differences are active and inert material. The more minor differences result from porosity and the ratio between the reactive part and the inert. The ratio is usually between 30–80 m-%. These concrete differences affect the properties the oxygen carrier has at reactions and the process.

Oxygen transport capacity is presented at oxygen per mole of metal. The capacity varies between 0.0096–0.67 moles of O_2 /mole metal depending on the oxygen carrier used. This does not tell us the whole truth about the feasibility of the oxygen carrier because of certain limiting properties. Thermodynamical properties are important for reactions and heat transfer.

The melting point of the oxygen carrier rules some oxygen carriers out of the CLC process. If process temperatures get near the melting point, the oxygen carriers start to get soft. Soft oxygen carrier wears faster and may get agglomerated, which decreases the circulation or may even block it. For example, Cu/CuO can be agglomerated due to intensive heat and Cd, Zn and Ce are not suitable for CLC at all, because they have a low melting point. (Hossain & de Lasa 2008)

Physical properties are important for other parts of the process as well. The fluidizability of particles is determined by density and particle size. Good fluidizability is necessary for controllability and circulation. Density and particle size also affect the overall reaction rate and the external and internal heat transfer of the particle. Crushing strength is important for the CLC processes where oxygen carrier recycles. The recycle of oxygen carrier increases physical stress. A process that does not use recycle, for example a rotating reactor (Håkonsen et al. 2010), may include less physical stress. (Hossain & de Lasa 2008)

There are three very promising oxygen carriers which are often compared in literature (Johansson 2007). Ni, Cu and Fe based oxygen carriers all have good and bad properties. Ni is the most reactive and thermally stable, but it is toxic and the most expensive. Cu has quite good reactivity but a low melting point, which may cause problems. Fe is less reactive, but it is cheap and easily available and can endure physical stress and heat.

Non-synthetic oxygen carriers could also be an option. The benefit of mineral, waste or ore based oxygen carriers is often the price. Usually the waste from metal industry is cheap when compared to synthetic oxygen carriers. One well examined oxygen carrier is ilmenite, $FeTiO_3$, which has been under large surveys (Rydén et al. 2009).

Another interesting option that also derives from metal industry waste is the use of iron oxide scales. Rydén et al. (2009) points out that iron oxide scales have no or very little economical value. Iron oxide scales are produced as by-product during the rolling of metal sheets. Scales contain very small amounts of Si, Mn, Al, Ca and

P. The only thing needed for their preparation is the removal of residual oil from the process by heating.

The purpose of a good inert material is to support the reactive material, make particles moredurable and increase fluidizability. The inert materials are SiO₂, TiO₂, ZrO₂, Al₂O₃, YSZ and betonite (Hossain & de Lasa 2008). If the inert material is an oxide, it will affect the oxygen ratio (Zafar et al. 2006). Another important role for the inert is to be porous support for the metal oxide. This will increase the surface area for reaction. (Adánez et al. 2004, Ishida & Jin 1994, 1996)

2.3.1 Reactions of metal oxides

Reduction and oxidation reactions are essential for the process. Active metal of oxygen carrier is usually made from Cu, Ni or Fe. Basic reactions in the process with these metals are presented at Table 1.

All these reactions are possible at the process. The sum of reaction heat is constant and is not dependent on the reaction route. With Fe and Ni, the reaction with CH4 is endothermic, but all reactions with Cu are exothermic. R_0 presents oxygen ratio, calculated at Eq. 4. R_0 values at the table are for oxygen carrier which has 100% active metal.

2.3.2 Preparation of particles

Oxygen carriers can be produced in different ways and thus the quality of the CLC process varies. Good preparation makes it possible to use stiff, well reacting and uniform particles.

Freeze-granulation, impregnation and spray-drying are the main methods of producing oxygen carrier particles. Impregnation and spray-drying already are in commercial use.

Freeze granulation is used to make spherical particles with good strength. The disadvantage of this method is that it is not economically feasible (Johansson 2007). It can be used for lab-scale testing. Rydén et al. (2009) supports Johansson's (2007) opinions. If freeze-granulation could be done economically, it would be the best

		\mathbf{R}_0	ΔH_c^0 (kJ/mol)
CuO/Cu		0.20	
	$CH_4 + 4 CuO \Leftrightarrow 4 Cu + CO_2 + 2 H_2O$		-178.0
	$H_2 + CuO \Leftrightarrow Cu + H_2O$		-85.8
	$CO + CuO \Leftrightarrow Cu + CO$		-126.9
	O_2 +2 Cu \Leftrightarrow 2 CuO		-312.1
Fe2O3/Fe	2304	0.03	
	$CH4 + 12 Fe_2O_3 \Leftrightarrow 8 Fe_3O_4 + CO_2 + 2 H_2O$		141.0
	$H2 + 3 Fe_2O_3 \Leftrightarrow 2 Fe_3O_4 + H_2O$		-5.8
	$\text{CO} + 3 \text{ Fe}_2\text{O}_3 \Leftrightarrow 2 \text{ Fe}_3\text{O}_4 + \text{CO}_2$		-47.0
	$O2 + 4 Fe_3O_4 \Leftrightarrow 6 Fe_2O_3$		-471.9
NiO/Ni		0.21	
	$CH_4 + 4 NiO \Leftrightarrow 4 Ni + CO_2 + 2 H_2O$		156.5
	$H_2 + NiO \Leftrightarrow Ni + H_2O$		-2.1
	$\dot{CO} + NiO \Leftrightarrow Ni + \dot{CO}_2$		-43.3
	$O_2 + 2 \operatorname{Ni} \Leftrightarrow 2 \operatorname{NiO}$		-479.4
Other			
	$CH_4 + 2 O_2 \Leftrightarrow CO_2 + 2 H_2O$		-802.3
	$H_2 + 0.5 O_2 \Leftrightarrow H_2O$		-241.8
	$\text{CO} + 0.5 \text{ O}_2 \Leftrightarrow \text{CO}_2$		-282.9

Table 1. Reactions of the metal oxides used in CLC, oxygen transport capacity of the materials, R_o , and combustion heat at standard conditions (298.15 K, 0.1MPa) (Abad et al. 2007)

way to produce particles. Pore volume can be adjusted with process conditions. High surface area with controlled porosity can be obtained by freeze drying (Tallón et al. 2007).

de Diego et al. (2004) have noted that impregnation has some advantages. They were using titania and silica as a support and Cu as an active metal. The carrier had high reactivity and completed full conversions at test. Additionally, carrier particles maintained chemical and mechanical properties well, which makes impregnated carriers a good candidate for CLC.

Spray drying is a well known industrial scale technique. It has been used in food and pharmacy industry. Jerndal et al. (2009, 2010) have investigated these methods at several studies. They have mentioned that it is possible to make similar particles as freeze-granulation preparated. Difference between freeze-granulated and spray- dried particles is sphericity. Spray-dried particles have a hollow interior.

	Particle size	Sintering temperature
Crushing strength	Positive correlation	Positive correlation
Porosity	No correlation	Negative correlation
Density	No correlation	Positive correlation
Reaction rate	No correlation	Negative correlation
Surface area	Positive correlation	Negative correlation
Surface area/mass	Negative correlation	Negative correlation

Table 2. Effect of particle size and sintering temperature on particle properties

Spray-dried particles probably have lower crushing strength (Adánez et al. 2004). Additions of MgO and Ca(OH)₂ can increase physical strength. It is believed that the additions result in the formation of inert spinels $MgAl_2O_4$ and $CaAl_2O_4$ (Jerndal et al. 2009).

Sintering temperature affects the bind of the inert and the oxygen carrier. The increase in sintering temperature or time increases density, crushing strength and decreases porosity (Adánez et al. 2004). The sintering temperature and time depend on the inert, metal oxide and wanted properties. Sintering is usually done at temperatures between 950–1600°C, and sintering time usually has been six hours. If the sintering temperature is too high, the particles become deformed. The additions mentioned earlier increase the endurance of particles. (Johansson 2007)

The effects of sintering temperature on density, crushing strength, porosity and reactivity can be explained. In sintering, small scale deformation of the particle takes place. Small cracks and pores merge, which decreases porosity and increases density. Reaction rate is dependent on the surface area and porosity increases the effective surface area. Crushing strength is dependent on the density and structure of the particle, and low porosity makes the structure denser.

Mixed-oxide carriers are a combination of at least two different metals which are suitable for oxygen carriage. Mixed-oxide carriers are a possibility if we want better reactivity and strength. However, there is very little research done on the subject and only a few articles can be found. Despite this, the results can be seen as promising. Ni-Cu oxygen carrier can have good reactivity and good strength properties. Over 4% NiO at the oxygen carrier stabilizes the CuO phase and makes it possible to use it at 950°C (Adánez, García-Labiano, de Diego, Gayán, Celaya & Abad 2006).

Table 2. shows how particle size and sintering temperature affect particle properties. When particle size decreases, the surface area compared to mass increases. Particle size and sintering temperature provide an inconsistent effect on the oxygen carrier. This makes the oxygen carrier design challenging, and it is often hard to make compromises between the costs, reactivity and crushing strength.

Linderholm et al. (2010) have introduced three different oxygen carriers at the same process. They discovered that oxygen carriers with different properties support each other. Oxygen carrier mixture may increase conversion rate of the fuel. The survey also demonstrated that well working particles can be made from commercial materials and with methods that have realistic costs.

Gibbs energy is used for evaluating how reaction may occur and whether there is potential for full conversion of fuel. Gibbs energy presents the thermodynamic potential of a compound. At reactions, energy will be released or captured to compounds. Jerndal et al. (2006) have made a very profound analysis between oxygen carriers. Analysis shows that Mn_2O_3/Mn_3O_4 , CuO/Cu₂O, Fe₂O₃/Fe₃O₄ and NiO/Ni can convert methane to CO₂ almost completely.

2.3.3 Oxygen carrier experiments

The mapping of suitable oxygen carriers has been done quite systematically. Basic dependencies have been discovered during surveys. Dependencies cannot be predicted yet. Experiments have been made from physical, thermodynamical and chemical points of view. They all differ a little from each other.

Physical experiments have focused on how preparation affects to the physical properties of the particle, for example the crushing strength, porosity, density and the surface area. These properties can change a lot depending on the manufacturing method described earlier. What is important within the physical experiments is to test how well particles can handle multiple oxidation-reduction cycles and how they affect affects to physical properties of the oxygen carrier.

Thermal experiments look for information on thermal properties, such as the melting point and temperature derivation. Thermal interactions at reactions between other components of process have been under research. Heat transfer abilities have been studied because the oxygen carrier transfers heat between reactors. Oxidationreduction cycle changes the temperature in the particle at least two times per cycle. This causes stress to the particle.

Garcìa-Labiano et al. (2005) have made very comprehensive analysis and calculations about what kind of temperature variation can happen at the particle. The analysis takes into account the reaction type, inert material, metal weight fractions, porosity, kinetic parameters, external heat exchange and particle size.

Temperature variation at particle is important, because if the temperature increases too much, sintering and agglomeration can happen. The maximum temperature of the particle and how the temperature varies inside the particle can be calculated. In exothermic reactions temperature increases faster than in endothermic reactions.

Inert material, which is usually porous, is support for metal oxide. Heat distribution at the inert material is controlled by thermal conductivity, heat capacity and solid density. Inerts have relatively low thermal conductivity. Maximum temperatures follow sequence $ZrO_2>TiO_2>Al_2O_3>MgO>SiO_2$. Depending on the oxygen carrier temperature, derivation can increase inside the particle to over 90°C. García-Labiano et al. (2005) point out that the inert material has hardly affected the heat balance inside the particle.

The ratio of inert and active oxide material is a compromise. Wanted oxygen carrier capacity, crushing strength and costs are often rival properties. The price between metal oxides varies. Weight fraction balances between these. An important part to be taken into account is the heat transfer between reactors. The oxygen carrier transfers heat from the air reactor to the fuel reactor.

Clear correlation between metal weight fraction and crushing strength has not been found. Depending on the inert and metal oxide the results differ a lot. Nevertheless, clear positive correlation between sintering temperature and crushing strength can be found. An exception to this is that some compositions lose their strength at high sintering temperatures. (Adánez et al. 2004)

As can be seen from Table 3., porosity and crushing strength are negatively correlating properties. Reaction rate increases when particle is porous because gas diffusion resistance gets lower in the pore system. An interesting observation to particle maximum temperature difference and porous ratio can be seen at Fig. 3 When porosity gets over 0.4, conversion speed decreases as it is supposed, but temperature difference at the particle decreases. (Garcìa-Labiano et al. 2005)

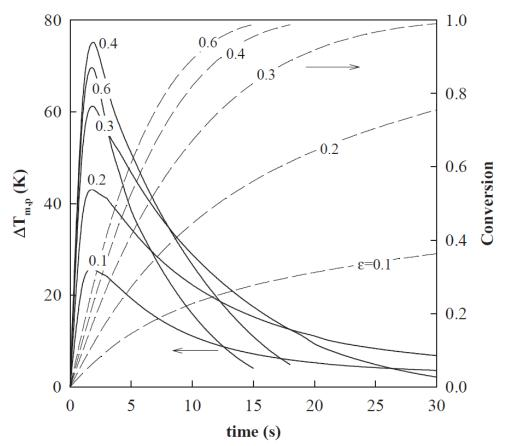


Figure 3. Effect of porosity on the maximum temperature increase inside of the particle during the Ni oxidation. (Garcia-Labiano et al. 2005)

It would be interesting to see how crushing strength would change between porosities 0.3–0.6 to this particle. Optimal porosity depends on the reaction rate, crushing strength and heat control.

At Fig. 4., it can be seen that when particle size increases, reaction rate decreases, but the temperature difference inside the particle increases. When the model has been run with isothermal conversion, difference to non-isothermal does not change dramatically. Garcia-Labiano et al. (2005) claims that main resistance at heat transfer comes from the film heat transfer and that conversion calculations for isothermal particle models can be used.

... under the typical conditions present in a CLC system, with particle sizes lower than 0.3mm, 40 wt% of metal oxide content, and full reaction times of 30 s, the particles can be considered isothermal and the heat balance can be ignored to model the reactions. (Garcìa-Labiano et al. 2005)

	Crushing strength	Porosity
Particle size	Positive correlation	No correlation
Sintering temperature	Positive correlation	Negative correlation
Crushing strength	-	Negative correlation
Porosity	Negative correlation	-
Density	Positive correlation	Negative correlation
Reaction rate	Negative correlation	Positive correlation
Surface area	No correlation	Positive correlation
Surface area/mass	No correlation	Positive correlation

Table 3. Contradiction between crushing strength and porosity

This serves as a guideline of what kind of accuracy is needed for reactor design. Particles with high metal oxide content can be handled as isothermal.

Johansson (2007) has made a general conclusion of what the oxygen carrier research has discovered:

- 1. Most reactive oxygen carriers contain nickel and copper oxides as active material.
- 2. Copper is easy to de-fluidize and agglomerate
- 3. Nickel oxide has limitations to convert fuel gases fully to CO_2 and H_2O
- 4. The reduction reactivity is faster for syngas (H $_2$ and CO) as fuel than with CH_4
- 5. Reactivity increases reaction temperature, high reactivity has also achieved with relatively low temperatures.
- 6. No real correlation between particle size and reactivity has been established

I partly disagree with Johansson (2007) conclusion that particle size does not affect reactivity. In Fig. 4, it can be seen that smaller particle size increases conversion which depends on reactivity. However, it can be seen that the difference in conversion gets smaller when particle size decreases after 0.3mm.

N-VITO is oxygen carrier particle which has been made at Flemish Institute for Technological Research. Snijkers et al. (2010) mentions that this particle is spray

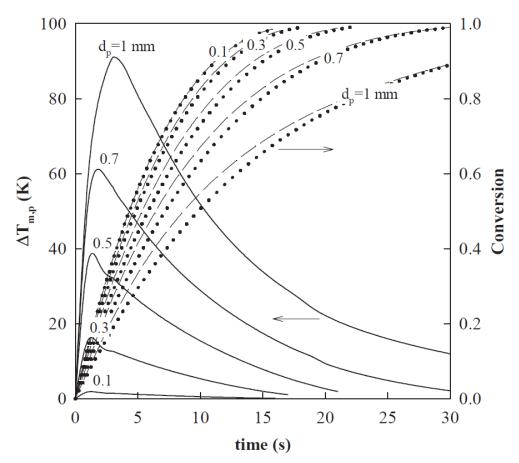


Figure 4. Effect of particle size on the solid conversion and the maximum temperature increase inside of the particle for the Ni oxidation reaction (dotted line = isothermal particles). (Garcìa-Labiano et al. 2005)

dried and is combination of NiO/NiAl2O4. Because particle is made with method for industrial scale, N-VITO is interesting particle for testing different reactor systems. N-VITOMg is oxygen carrier which has additional Mg for increasing reactivity. Linderholm et al. (2009) have used N-VITO as reference particle at their research.

2.4 Process designs

Experiments can also be divided between process concept and reactor design for testing oxygen carriers. Reactor design is mainly oriented towards oxygen carrier testing. Reactor design tries to enable the possibility of testing multiple oxygen carriers fast, reliably and cheap.

Process design and experiments lean to knowledge and support of combustion and

gasification in fluidized beds. Fluidized beds have been known since the early 20th century and have been under research for a long time. Now the same application is utilized for new technology.

Deep analysis about process or reactor designs does not exist in literature. A possible reason for this is perhaps that reactor and process design are key knowledge at research facilities. Good reactor design makes it possible to get ahead other facilities when it comes to research.

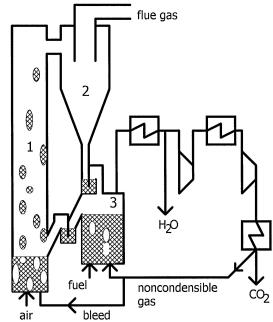
2.4.1 Reactor designs

Experimental reactor designs are divided into hot and cold flow models. Main difference is the working temperature. In the cold flow models, the temperature is ambient temperature, and no reaction occurs. Metal oxide particles in cold models are often replaced with glass, sand or polymer particles which are more stable (Riehle 2000). Cold models are usually made from polycarbonate glass because it is relatively easy to construct and supervise. Cold models are more versatile in testing different flow models or reactor designs. Cold models are less expensive for testing purposes than the hot model, but they cannot be used in tests with reactions.

The idea of the cold models is to get answers and preliminary study on flows. Flow conditions of hot models can be evaluated, even if particles do not have the same properties as real oxygen carriers do. An important part of the reaction design is to know circulation rates and pressure differences with different flow velocities. Velocities and circulation rates can be calculated from measurements.

Hot model design differs from cold model design in many ways. Main differences are that reactions take place at reactors, it is not possible to monitor the flow by vision and hot models are usually heated with an outer source. Usually reactions at test equipments do not generate enough heat for a robust process. External heat source is needed to keep reactions running and the temperature constant, which increases the possibility of carrying out comparable tests.

Particle locks are often tested with cold models to prevent gas leakage between reactors. Smooth particle flow is essential for a robust and a stable process which is monitored through the walls of the cold model. Particle locks increase solid inventory at process. Well planned particle locks can decrease the amount of solids



needed, which decreases costs particularly in tests.

Figure 5. Reactor design presented by Lyngfelt, 1. Riser of air reaction, 2. Separation cyclone 3. Fuel reactor. (Lyngfelt et al. 2001)

Construction itself has been kept as similar as possible. One of the earliest reactor designs produced is interconnected fluidized beds (Lyngfelt et al. 2001). The design which Lyngfelt et al. (2001) have presented to literature can be seen at Fig. 5. Lyngfelt mentions that this design has the advantage of producing good contact between gas and solid phase, which is essential for the process.

The design contains two reactors, air and fuel. Air reactor continues to a riser which can be narrowed. After the riser, the flow goes to a separation cyclone which separates the oxygen carrier and oxygen depressed air. Oxygen carrier particles drop to the particle lock which prevents CO_2 from leaking into the separator. This would decrease CO_2 recovery because the outlet from the separator goes directly outside without recovery. After the particle lock, the oxygen carriers drop to the fuel reactor due to gravitational forces. After the reaction, the oxygen carriers go through one particle lock and drop back to the air reactor. The fuel reactor is located at a higher level than the air reactor.

Literature knows multiple other designs as well. Main differences between the designs are the number of cyclones and the differences at loops. Recycling loops can be done to air or fuel reactor. These loops are presented at Fig. 6. The advantages

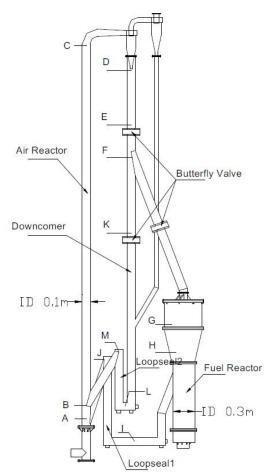


Figure 6. Reactor design with recycle loops. (Xu et al. 2009)

of these loops differ between reactors. At an air reactor loop, the share of particle flow is recycled to the bottom of the reactor. The purpose of this loop is to increase the oxidation of oxygen carrier in the air reactor by increasing the average residence time. The residence time alters between designs, and often it is too short (Xu et al. 2009). Another advantage is that higher solid conversion with higher gas velocity can be achieved at riser. This implementation also increases the controllability of the total process because adjusting the particle flow enables better control of the fuel reactor.

Loops at fuel reaction can be made in at least two different ways. First option is to divide the oxygen carrier stream which goes to the air reaction, and the second option is to recycle part of it to the fuel reactor. The latter will increase the average residence time of oxygen carrier in the fuel reactor. Surveys have concluded that oxygen carrier is not fully reduced in reasonable time after the fuel reaction. With this loop, the reduction reaction will continue a little longer. This will increase the effective oxygen load of oxygen carrier at the system. However, it is not always preferable to reduce the oxygen carrier all the way, because of differences between the multiple oxidation levels. Oxidation levels alter between oxygen carriers. Second option is to recycle part of the combustion gases from the fuel reactor. This may be useful if the fuel is not fully burnt out. For good efficiency, there should be no fuel gas leak to CO_2 processing.

Cyclones separate the solids and the gas flow at reactor outlet. Cyclone design and sizing is relatively trivial, and there are several generally approved methods to size a cyclone. Parameters that are needed are from solid and gas properties and from the parameters from the flow which is introduced to the cyclone. Solids which are used at CLC-process are still expensive, which increases the value of efficient separation.

Loop seals are an important part of the separation process between gas volumes in reactors. If gas volumes are not well separated, gas leakage may occur, which will decrease the efficiency of carbon capture. Loop seals are controlled with air or steam flow at the bottom of the loop seal, and pressure difference between reactors. Basu & Cheng (2000) have presented comprehensive analysis on loop seals. Loops system only operates correctly at a certain range of aeration which is connected to riser gas velocity. This is very important and has to be taken into account when a reactor is going to be designed. Loop design varies depending on particle size, density, preferred circulation rates and pressure differences between sides. (Basu & Butler 2009)

At the reactor, solids make regions. Usually regions are divided into two. The lower region is called a dense bed or a bottom bed, and the higher level a dilute region or a freeboard. Johnsson et al. (1991) has modified the theory of the dense bed. The dense bed is divided as follows: 1) region with minimum fluidization velocity, 2) region of visible bubble flow. A dilute region starts after these regions. The properties of the regions are different. At a lower region, gas transference is limited. Reaction rate increases at the dilute region because gas-solid contact is better. (Abad et al. 2010)

Reactor design can start from several points of view. The point of view specifies which properties will be fixed and which can be defined during design. For laboratory scale, determinants are usually solid inventory, power scale and size. This is because in laboratory tests, multiple different oxygen carriers are used and tested. Test matrix generally gets cheaper if the needed solid inventory can be decreased.

The power scale is connected to the solid inventory. More oxygen carriers are

needed if more power is wanted because more fuel has to be burned. Solid inventory can be divided into two parts, an active part and a burden part. The active part of the solid inventory participates in reactions and the burden part moves between reactors or is deposited in particle locks.

The active part is important for power and the burden part is important for a robust process. The burden part can be decreased as long as particle locks work or gas leakage does not occur. The amount of solid inventory changes the size of components via optimal velocities.

Free settling velocity of particle is defined by particle properties. It is important that particles are entrained with gas at the riser. If gas velocity is not high enough, solid particles will not be entrained and solid flow stops. Velocities are also affected by pressure drops during process. Correct pressure differences are essential for a robust process. If pressure difference is not correct especially between reactors, particle locks will not work properly and gas leakage will happen.

The needed residence time for the reaction to reach the wanted conversion can be defined from the reaction rate and parent substances. Usually this is calculated or simulated time dependent. The idea is that the oxygen carriers are in the reactor until the wanted conversion rate is obtained. Average residence time and average particle size is often used for calculations, because particle size distribution varies between oxygen carriers, manufacturing methods and during process.

Side-plots at design are cyclones and heat exchange from reactors. These support the process and make it more reliable. Heat exchange design mainly depends on the physical properties of the equipment and the heat which comes from the process.

Component and reactor sizes are defined from the wanted design, solid and fuel properties, free settling velocity, residence time and solid inventory. The properties of the oxygen carrier and fuel are necessary to know for the reactor design. The design process can begin with the wanted power, mass of active solid, maximum inventory of solids at the process or the size of the equipment. Some of these should be fixed for initial design. Other design properties are connected to these.

The design process is usually iterative, especially when what is looked for is an optimal design for profitable power production. It is possible to minimize the costs if the connection between the design properties and costs can be determined.

2.4.2 Experimental reactor design

Reactor design experiments are divided into cold and hot model experiments. Cold models are first made to assure solid flow and to inspect hydrodynamics at fluidized bed. After this, hot models are used for reaction testing. These testing reactors usually function at low power level, under 1kW and are externally heated. Also air and fuel reactors might be combined into one structure.

Chong et al. (1986) introduced a simple, small size design. It was made for char production without gas mixing. Reactor design was more deeply analyzed by Fang et al. (2003). This kind of design is increasingly used by Chalmers University of Technology during oxygen carrier tests. The design is illustrated at Fig. 7.

The reactor works well if solid transfer is sufficient between reactors. Even if the reactor is fully heated by an external source, it is essential that the oxygen carrier circulates heat to the fuel reactor where the endothermic reaction takes place.

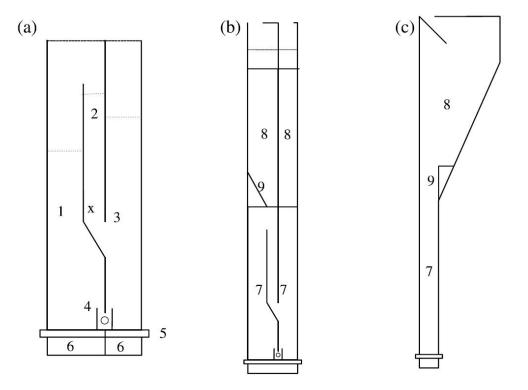


Figure 7. (a) the lower part, frontview, (b) entire reactor, frontview, (c) entire reactor, sideview.

The principal sketch of the reactor: (1) air reactor, (2) downcomer, (3) fuel reactor, (4) slot, (5) gas distributor plate, (6) wind box, (7) reactor part, (8) particle separator, (9) leaning wall. Fluidization in the downcomer (x) and slot (o) is also indicated. (Abad et al. 2006)

Small improvements have been introduced by Rydén et al. (2008). The design at downcomer and the return orifice have changed. The purpose of this is to reduce CO_2 dilution to fuel reaction. These improvements can been seen at Fig. 8. Inlets for air and fuel come from bottom and outlets are at the top.

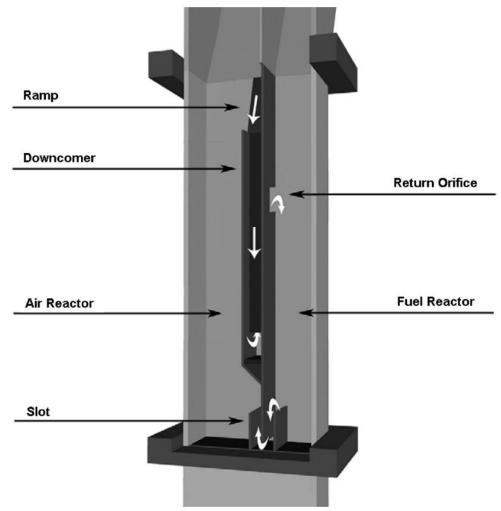


Figure 8. Schematic description of the improved reactor for oxygen carrier tests. (Rydén et al. 2008)

Adánez et al. (2009) have presented a reactor setup which is between earlier 300W reactors and concept scale. The reactor works at 500W power. The reactors are separated and temperature is controlled with two furnaces. Typically solid inventory is between 0.8–1.5kg depending on the density of the particles. At tests solid inventory in the fuel reactor was 0.3kg and at 0.5kg in air reactor.

It is mentioned that experiment construction was easy to operate and maintained stable conditions during tests. This was validated with multiple repeated tests. The

tests had similar results. (Adánez et al. 2009).

This construction is very promising and combines oxygen carrier testing and the possibility of validating models for full scale systems. The schematic design of Adánez et al. (2009) can be seen at Fig. 9. Construction is very near the propositions of full scale reaction schematics.

Low power reactors which are designed only for oxygen carrier testing can be even simpler. One of the simplest reactor designs is a quartz pipe which contains porous grate for oxygen carrier bed. Air, inert gas (for example N_2) and fuel flows are introduced to reactor at sequences. Temperature and pressure measurements are made and exhaust gas is analyzed.

These reactors are suitable for determining what kind of reaction rates are reasonable to be expected at full scale process and whether carbon deposit appears at particles. With this kind of technique, oxygen carrier particles are also tested for suitability for different kind of fuels.

2.4.3 Concept scale design

The purpose of concept design is to test reactor designs which could be suitable for a full scale unit. Concept scale reactors are usually separated and more powerful, over 5kW. Concept scale reactor may have recycling loops for adjusting particle flow. Opposite to reactors which are meant for oxygen carrier testing, flow is usually controlled only with flow rates at reactors. Concept type reactors are not covered very well in literature. There is a clear gap in literature when it comes to concept type research. This will be one of the goals that future research might aim to achieve.

Also comparison between different kinds of reactor designs lacks from the literature. Several standard and commercial research particles are introduced but surveys with the same particles at different reactor designs cannot be found in literature. This makes reactor design surveys less comparable.

Also comparisons between different kinds of reactor designs lack from literature. Son & Kim (2006) have presented a concept which includes a double loop and where the air reactor is inside the fuel reactor. Reactor schematic diagram is at

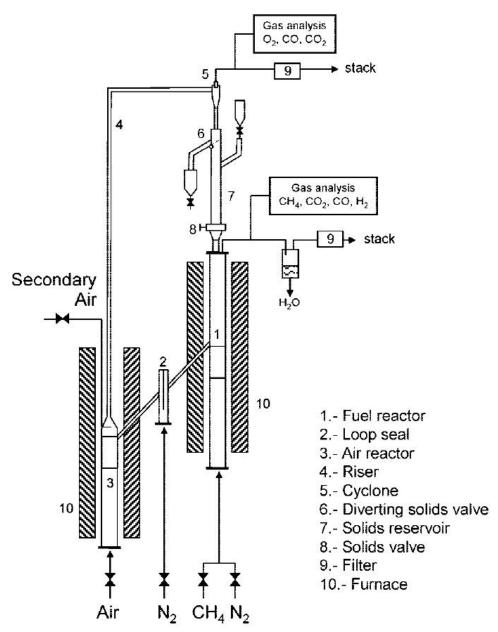


Figure 9. Schematic description of 500W reactor. (Adánez et al. 2009)

Fig. 10. This concept is unique and the study has been cited and noticed also in literature. However, there is no further investigation about the concept in literature. The power of the reactor is not known, but solid inventories are 0.2 kg at the air reactor and 0.6 kg at the fuel reactor. This indicates that the power is relatively small, between 0.5-1.5 kW.

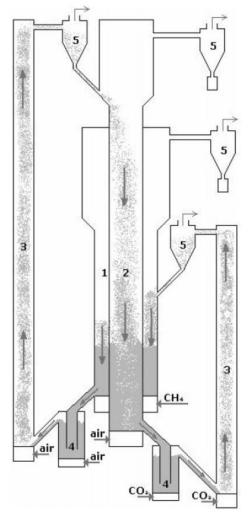


Figure 10. Schematic diagram of CFB reactor for CLC. (1) Reduction zone, annular column, 55 mm i.d., 0.9 m height; (2) oxidation zone, inner column, 23 mm i.d., 1.5 m height; (3) riser, 17 mm i.d., 2.1 m height for oxidizer, 1.15 m height for reducer; (4) loop-seal, 23 mm i.d., seal-pot type; and (5) cyclone.

Before the 300W reactor at Chalmers University of Technology, Lyngfelt et al. (2001) presented the first sizing and reactor model for a 10kW reactor. The article also examined the relationship between carrier properties and design data. Design is an iterative process where properties affect each other. These relationships can be seen at Fig. 11. Initial design of 10kW reactor is based on these dependencies.

This was the first reactor setup that was used for chemical loop combustion with particle circulation. It can be assumed that the first prototype does not have a fully optimized design, therefore the design only gave guidelines for future design. Schematic for initial design is presented at Fig. 5.

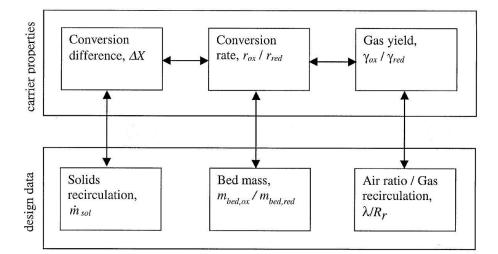


Figure 11. The basic relations between carrier reactivity and design input data. (Lyngfelt et al. 2001)

Already at an early stage, Vienna University of Technology and Chalmers University of Technology collaborated with the 10kW reactor (Lyngfelt & Thunman 2005). Dimensioning and a cold model were produced in Vienna. The cold model and dimensioning are presented in literature by Kronberger et al. (2004). The design procedure of dimensioning and design is presented at Fig. 12.

Only a few years later, two surveys connected to this reactor type (Lyngfelt et al. 2004, Lyngfelt & Thunman 2005) were presented. During those few years the reactor was built and over 100 hours of testing had been done. Lots of interesting and useful knowledge was attained from those first tests. Lyngfelt & Thunman (2005) mentions that the overall operation was stable and the process could be run for long periods of time without modifications such as gas flow adjustments.

Two things which relate directly to chemical loop combustion are also mentioned: fluidization velocity of the particle locks is essential for particle circulation and after extended operation time, smaller size of particle distribution were lost from separation. Fluidization velocity should be adjusted higher for the upper particle lock in order to prevent the particles from gathering to the cyclone and circulation would more likely stop at the bottom particle lock.

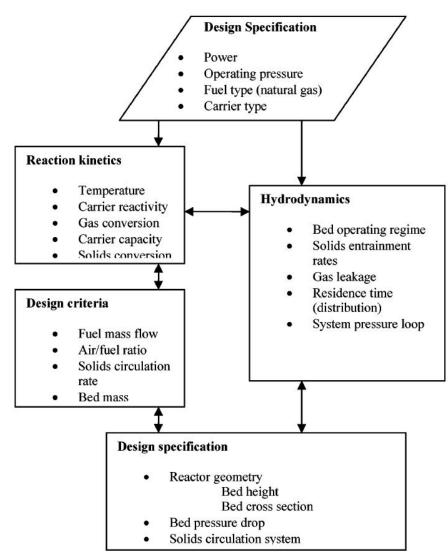


Figure 12. Design procedure of a chemical-looping combustor. (Kronberger et al. 2004)

After these surveys, long combustion time surveys (Adánez, Gayán, Celaya, de Diego, García-Labiano & Abad 2006, Linderholm et al. 2008, 2009) have been introduced in literature. Knowledge from preliminary studies has increased. Process is robust and easily controlled which has increased runnability. These things enable the testing of long term suitability of the oxygen carrier. Some of these tests use the N-VITO and N-VITOMg particles mentioned earlier (page 32.), which makes the results more comparable.

A chemical-loop combustion system that works at 50kW power has been built at Korea Institute of Energy Research (Ryu et al. 2004). The construction of the system includes small differences compared to the 10kW combustion system. A reactor bed is controlled by a valve at the bottom of the reactor. In some other designs, the rector bed level is constant. Difference at schematics can be seen when Fig. 9. and

Fig. 13. are compared.

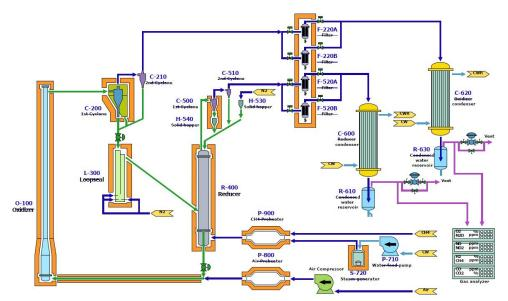


Figure 13. Schematic diagram of a 50kW_{th} chemical-looping combustion system. (Ryu et al. 2004)

The advantage of this kind of a reactor bed control is that it makes it possible to adjust bed height and circulation of solids. It is certain that the optimal bed height depends greatly on the oxygen carrier used. This design enables the research on optimal bed height and circulation rate. Ryu et al. (2004) emphasize that stable pressure drop has to maintained at the process. This is essential for smooth solid circulation.

Chemical-looping combustion system of 120kW was built at Vienna university of technology in 2007 (Kolbitsch, Pröll, Bolhar-Nordenkampf & Hofbauer 2009). This reactor system is the first CLC system which attempts to fill the gap in scale up research. Combustion system is based on the idea of dual circulating fluidized bed. There are two reactors which are usually only seen at an air reactor. The aim of this design is to use the whole reactor volume for reaction. The fuel reactor has an internal loop which can be seen at Fig. 15. The setup uses three loop-seals, upper, inner and lower. These loop-seals control the solid flow and separate gas space.

Before the hot model, Pröll et al. (2009) constructed a cold flow model from dual circulating fluidized bed. The article includes comprehensive description used for scaling parameters. Pröll et al. (2009) notes that several dimensionless ratios are important for scalability. Re_p , Ar, Fr, gas/particle density ratio, reactor/particle

diameter ratio, reactor diameter/height ratio, particle sphericity and particle size distribution where used for scaling. Good scalability is achieved using these similarities.

Pressure measurements show that all particles do not go through the internal loop at the fuel reactor. There is no accurate data on how the loop is introduced back to the fuel reactor, but solid flow is probably introduced to annulus region at reactor. This region can be seen at Fig. 14. This way, smaller amount of already reduced oxygen carrier circulates in the fuel reactor.

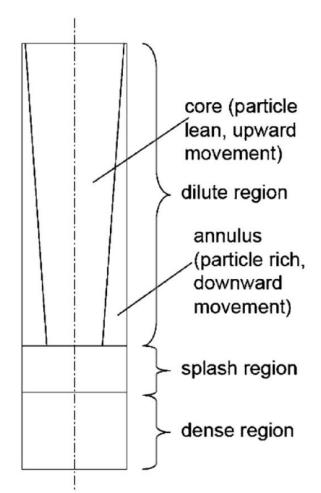


Figure 14. Typical structure of fluid dynamic description of fast fluidized bed reactors Kolbitsch, Pröll & Hofbauer (2009)

DCFB has a couple of advantages compared to other concepts. Solid circulation is fast and solid-gas contact is effective, which decreases solid inventory. High solid circulation rate may decrease durability of oxygen carrier. Pröll et al. (2010) present that carbon formation does not occur if air/fuel ratio is high enough. They predict

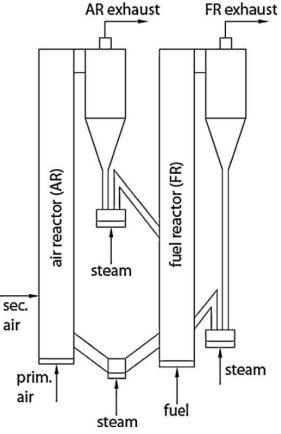


Figure 15. DCFB reactor system set-up. Both AR and FR are designed as circulating fluidized beds. Kolbitsch et al. (2010)

that next system power scale would be $10-20MW_{th}$.

Alstom Power Inc. has done production research and built several reactor prototypes. They have at least 15kW and 65kW reactor systems. The 15kW reactor was published in 2009 and the 65kW pilot plant has been tested at least from 2006 (Lyngfelt 2010). Construction is well integrated. All chemistry and reaction rates are verified.

Alstom Power has also built two cold flow prototypes which are made for scale-up and solid circulation research. Alstom has informed that by the end of 2010 and during the early months of 2011, $3MW_t$ CaS prototype is built and preliminarily operated (Abdulally et al. 2010). Also at end of 2010, the commissioning of $1MW_{th}$ plant, which uses metal oxides, will take place (Beal et al. 2009). $1MW_{th}$ plant will probably use schematics similar to Fig. 16.

Reactor schematic can be seen at Fig. 16. Size and circulation rates are unknown. Deeper information on reactors and the process used by Alstom Power Inc. cannot

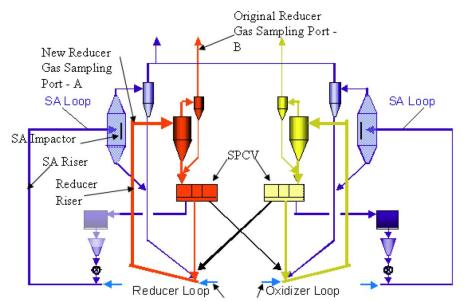


Figure 16. Schematics of reactor by Alstom Power Inc. (Abdulally et al. 2010)

be fully verified because the corporation does not want to distribute further knowledge.

Ryu et al. (2008) has introduced several different CFB process concepts. At Fig. 17., we can see some conventional CFB reactors and at Fig. 18., a reactor design with two risers. Main differences are that usually reactor design includes only one riser. Kolbitsch et al. (2010) have later used a bit similar design, but have added three particle locks to the system.

Two fluidized beds that use sequential flow are presented at Fig. 17c. Oxidating, fuel and inert gas are introduced to the reactors at sequences. Problem with this kind of a setup is pressure shock when the gas streams are switched. Ryu et al. (2008) note that reactors at Fig. 17a. and 17b. have 4-5 vessels when particle locks are included. This kind of a setup increases pressure drop and the complexity of the process which may produce problems to the sustained particle circulation.

Earlier systems are mainly for oxygen carrier research. 500W reactor, (Fig. 9)., which is capable to test oxygen carriers, possibility to scale-up research and model validation by Adánez et al. (2009), is a very tempting system set-up for research facilities.

DCFB reactor system, Fig. 17., by Kolbitsch et al. (2010), is the most promising one when it comes to commercial systems. The two bubbling bed interconnected

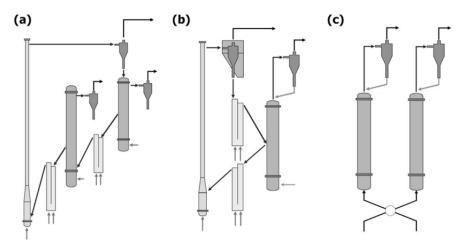


Figure 17. Schematic of conventional two interconnected circulating fluidized bed system. (Ryu et al. 2008)

CFB system, (Fig. 18)., by Ryu et al. (2008). is also promising.

2.4.4 Experiment arrangements

Experimental tests which are connected to reactor or CLC-process design focus on inspecting gas leakage, flow speed, circulation rates and total solid inventory. Oxygen carrier tests inspect more deeply the reaction rate, erosion of particles and loss of solids. Experiments can be made with air, CH₄, syngas-mixtures or natural gas depending on what kind of surveys are intended.

Some of the basic procedures are very similar in different experiments. The reactors are filled with oxygen carrier, air and inert gas start solid circulation and the reactors are heated to the desired temperature. Air functions as the gas for an air reactor circulation and nitrogen or car- bon dioxide as the gas for a fuel reactor. The operation is started this way because it will prevent generation of agglomeration or hot spots. Reactors warm up evenly and are ready for the reactions. After these steps, the inert gas is changed to the desired fuel. Depending on the degree of automation used, this can be done by steps or sliding control.

2.4.5 Design criteria

Design criteria are guidelines that lead design. They will guide the design so that the desired setup is achieved. Initial criteria for the design are usually pressure,

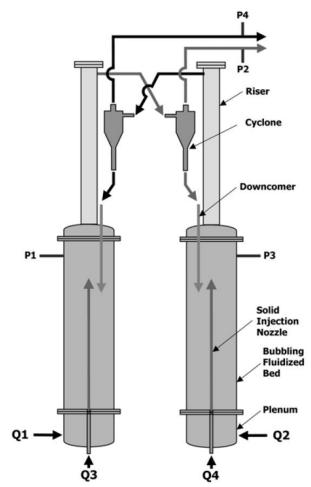


Figure 18. Schematic of a two bubbling bed interconnected circulating fluidized bed system. (Ryu et al. 2008)

nominal power and concept. These serve as a guideline for the design, all other selections aremade from this base. Designing is a bit of an iterative process, for example if the goal is to test oxygen carriers, the initial nominal power may be too high for reasonable solid inventory, which leads to an iterative process.

Approximation to reasonable nominal power can be calculated from the assumption that solid inventory is usually 500–1300 kg/MW for syngas and somewhat smaller for natural gas for solid circulating system (Abad et al. 2006). As mentioned earlier, it is essential to understand the relationships between the design parameters.

Additional selections are often made for design as the fuel which was used, oxygen carrier, air ratio, working temperature, recirculation rate and conversion differ. Some of these are connected to initial design criteria. Design parameters which also have to be taken into account are pressure drop, cross section of reactors and voidage. (Lyngfelt et al. 2001) After choosing or estimating the design parameters, more accurate parameters can be derived. This needs estimation or knowledge about oxygen carrier properties. Relationship between oxygen carrier and design input data can be seen at Fig. 11.

Conversion difference, ΔX , affects solid recirculation, which is also connected to heat transfer. Conversion rate, r_{ox}/r_{red} , affects bed mass. Solid inventory increases if conversion rate is low.

More detailed analysis of calculations is presented in section 3 on page 56.

2.5 Process modeling

Nowadays experiments are usually combined with computational models. Computational models are made for better understanding and prediction of the process. Viewpoint differs depending on how accurate a model is needed and what kind of information is wanted from the experiment.

A couple of CFD models were recently introduced in literature (Cloete et al. 2010, Jung & Gamwo 2008, Kruggel-Emden et al. 2010). Some models are capable of connecting combinations of models. The benefit of these models is that the combined models can give more accurate results because reaction and thermal models are dependent from momentum and mass transfer models.

These CFD models are used for reaction design and are more focused on where and how reaction takes place. This kind of study can reveal solutions to problems. Problem with CFD models is that when dimensions and variables increase, the models usually get more unstable and are harder to converge. CFD models are often made at transient model because fluidized bed reactor does not have steady-state solution.

2.5.1 Models

Computational models cover a vast range of models which are solved numerically. Often it is not possible to solve these models analytically. Commercial software does not support CLC process well because research is young and there is a lack of measurement data. In literature, most of the computational models are custom made, excluding CFD models. CFD models are easier to construct with commercial software.

The easiest way to model a reactor is to use a 1D model which presents how reaction concentration changes during time, place or both. These kinds of models can be done for example with Matlab or any software made for technical computing.

In the field of technical literature, reduction and oxidation models of oxygen carriers can be divided into two: i) nucleation and nuclei growth models and ii) unreacted shrinking core models. The main difference between these models is that in the unreacted shrinking core model the reaction rate is dependent on particle size and pore structure of a solid reactant. Nucleation model only considers chemical mechanism and kinetics between gas-solid reactions. This type lacks accuracy because grain size starts to have an impact when particle diameter is greater than 10 μ m, especially for porous particles. (Hossain & de Lasa 2008)

Jung & Gamwo (2008) have presented the first fluid dynamics modeling for CLC in open literature. The model deals with multiphase hydrodynamics of the fuel reactor. Survey concentrates on investigating how dense bed affects the reaction. Conclusion is that large bubbles can bypass dense flow region relatively easy, which may cause problems. The model contains only hydrodynamics and is isothermal. It was made with a commercial program.

Kolbitsch, Pröll, Bolhar-Nordenkampf & Hofbauer (2009) have modeled for fuel and air reactor with simplified structure which allows only a small amount of adaption. Model is coded with C++, which makes it possible to easily add more detailed sequences to the code. Shrinking core model is used for reactor kinetics.

The amount of CFD models has increased. Most models are made with commercial programs. Deng et al. (2009) have used FLUENT. CFD model uses momentum, energy and reaction kinematic equations. Multiphase model was solved time depended. Conclusions are similar to Jung & Gamwo: low fuel conversion rate due fast large bubbles.

A very interesting article on modeling is introduced by Balaji et al. (2010). This model tries to determine the most important physical and operating parameters of the CLC system. The model code was made with Matlab/Simulink. Simulation has been solved time dependently. It is based on thermodynamical equilibrium and it uses the shrinking core model. Chemical equilibrium is calculated by minimizing Gibbs free energy of gas species at system. Model is validated with concentration

measurements of gas species. Information on what kind of reactor design is used for validation is not available.

Bolhàr-Nordenkampf et al. (2009) have made a process model with IPSEpro. The process model is made with flow sheet simulation. The assumption that air and fuel reactor have constant temperatures has made it to the model.

Most of the models are from the fuel reactor, because it has been seen as the most critical component. Future models will advance to air reactor and cyclones. It is likely that 3D CFD simulations are made for the whole system before 2015. In the future, models should be made using such language and interface which can be adapted to create new, more accurate models. A general purpose graphical processing unit, GPGPU, based on calculation, will shake the world of modeling and simulations in the future. In order to revolutionize the field, more rapid models should be made ready for parallel computing.

2.5.2 Validation

An important part of modeling is validation. Validation is the part where the model is compared with the real world. It is important that the validation is done correctly. Approved validation is valid only within the range where validation has been done, which is good to know when the model is being used. There are several exceptions to this: some models can be used for scale-up, but that depends highly on the theory behind the model. As models use assumptions, there has to be some assumptions made also in the validation part of modeling. Usually these assumptions decrease accuracy, but not every issue concerning modeling and validation can be taken into account.

Usually validation is done by comparing measurements and calculations with the ones from the model. With same inputs, the outputs and measurements should be quite similar. Usually there is some variation between these two.

As mentioned earlier, the model by Balaji et al. (2010) was validated with measured gas concentrations. Relatively good agreement was found between model results and measurements. Despite the fact that agreement was found, there was doubt whether the heat equations worked properly because of absent heat radiation equations and the insulation assumption. At fluidized-bed, there are two separate sections, a dense bed and a diluted region. These two differ in fluid dynamics and reaction rates, which makes validation hard. Measurements for example for concentration can be difficult in these regions. Models can be used for designing and optimizing the CLC process when the models have been validated properly. (Abad et al. 2010)

One of the earliest validations for fuel reaction were done in 2009 by Abad et al. (2009). Experimental and predicted data were compared and good agreement was found. Model was validated with 10kW CLC prototype.

Process scale model was validated with 120kW pilot unit. Raw values from pilot unit are very near to equalized values from the model. Validation was made by gas concentration from outlets of air and fuel reactor. Bolhàr-Nordenkampf et al. (2009) reveal that the next step is to integrate the model to power plant layout in order to investigate the potential of the chemical looping process.

Even though validation is such a crucial part of modeling and model reliability, validation is not very well illustrated in CLC literature. In some cases it seems that validation is excluded because of expediency or it has been done, but not published. Research groups that can validate their model and introduce it in its entirety in open literature will certainly be noted.

3 MODEL

The aim of the model is to give assistance to design. The model calculates outlet values of gas and particle streams and the heat transfer needed to the reactor. The model solves problems as time dependent. The model can be verified with measurements when the reactor system has been obtained. The model does not include pre-existent calculation for the model.

3.1 Features and assumptions of pre-existing model

A pre-existing model has been made by J. Saastamoinen (Saastamoinen 2010). The pre-existing model simulates only air reactor reliable, and circulation between reactors is not applied.

Key features of the model are:

- One dimensional structure of the reactor
- Model takes into account the particle size, mass flow rates and particle inventories
- Simplified dimensioning model
- Equations are solved numerically.

Assumptions for the model are:

- Particle size is constant
- Particles are spherical
- Reactions do not take place at gas phase
- Particles are isothermal
- CH₄ reacts direct to CO₂
- Temperature of reactor wall is known and constant

• Gas flows are handled as plug flows.

All particles at system are mono-sized. This simplifies the model significantly. Gas flow is assumed to be plug flow and particles are following plug flow due to drag forces which are stronger than gravity.

The model may provide too optimistic results because in the model, CH_4 reacts direct to CO_2 . It is also possible that the reaction at combustion may also contain a part where CH4 is only partly oxidized to CO. This may happen especially when there is not enough oxygen in the combustion.

3.1.1 Model improvements

The model has been improved. For reactor design, it was essential to improve the model. Improvements have been made in order to increase accuracy, versatility and usability of the model. The improvements have been made when necessary and in case there was a noted fault in the model. More systematic model developments have not been made.

Model improvements:

- Capability of reliable modeling of the fuel reactor
- More accurate handling of gas density and viscosity
- Combined model of air and fuel reactor
- Calculation procedure of multiple oxidation-reduction loops
- Compiled inlet and outlet sheets for better usability
- Approximation of inventory, bed height and pressure drop at reactor
- Cross-checking the of model for more robust simulation
- Possible of parametric run for particle diameter, oxygen carrier mass flow and gas mass flow.

3.2 Model structure

The model has main equations which are modified depending on the assumptions. It has input terms which are imported to the system and the model gives provisional results and a final output.

First modification of the model calculates an entrained flow reactor, EFR. This represents a fast fluidized bed, for example a riser type air reactor. Main assumption for this modification is the bottom-up plug flow of gas. Particles follow the flow due to drag force.

Conversion and particle temperature are dependent on time. Gas temperature and mass fraction on species are dependent on location. Otherwise, equations and model structure are similar.

Oxygen carrier transfers heat between reactors. This transferred heat can be calculated when the temperature, mass flow of the oxygen carrier and the specific heat capacity are known. Usually gas which is introduced to the reactor is colder than the oxygen carrier.

The amount of external heating needed can be calculated from the heat loss from the reactor. The reactor part of the model is defined earlier as boundary conditions of the model. The defined parameters are reactors flow cross section area, cooling conductance, effective radiation factor, effective wall temperature and reactor height.

If flow cross section area of the reactor is to change, particle and gas velocities will change. Other parameters have more effect on the energy balance. Increase of height increases the retention time.

Material reactivity properties for different gases are taken from literature (Abad et al. 2007). Simple calculations for adjusting the model to right scale are also guided by the same article. Support for predefined parameters and preliminary calculations are made using an article by Lyngfelt et al. (2001).

Equations and main variables at model are presented at Fig. 19. Notice that multiple equations are calculated simultaneous and iteratively. Most of the equations are connected to each other. Changing a single parameter or variable may significantly

➡ Gas 쀖 Particle Particle mass (conversion) Eq. 27. m_p, m_g, m_i, X Gas mass (flow rate) Eq. 32. m_p, m_g, m_i, X Particle/gas energy Eq. 35., 38. T_w, T_g, T_p, Φ, Χ Particle Heat transfer Eq. momentum 35., T_w, T_g Eq. 30. w_p x, t Particle Gas

affect the entire calculation.

Figure 19. Main equations and variables at model

Reactivity and other properties for the model can be seen at Table 5. Material reactivity properties are from article Abad et al. (2007).

Fig. 20. presents the model structure and phases of simulation from initialization to post-prosessing. First initialization is based on initial conditions and oxygen carrier properties which are used as input. Fuel and air reactors are simulated at loop. Based on those simulations, output and cross-checking are carried out at postprocessing. If cross-checking gives values which are not in line with the initial

Material	Fe	Cu	Ni
Density, kg/m ³	3220,74	1773,28	2953,59
R	0,0198	0,0201	0,0856
Specific heat, when x=0, J/kgK	1040,44	1197,52	1033,66
Specific heat, when x=1, J/kgK	1013,4	1207,2	1058,6
$\mathbf{m}_r ed/\mathbf{m}_o x$	0,9802	0,9799	0,9144
Density at inlet, kg/m³	3274,86	1803,24	3085,16

Table 4. Oxygen carrier physical properties

conditions, input parameters are adjusted for the next simulation. Model is run iteratively until wanted or suitable results are obtained.

3.3 Mass transfer

Mass transfer at model is separated between gas and solid phase. Gas and solid phase interact at the surface of the particle where mass transfer takes place. Mass change binds the gas phase and the solid phase together.

Particle mass will change during oxidation and reduction reactions. Mass change comes from oxygen which is absorbed to the particle or desorption of oxygen from the particle. Mass transfer coefficient controls the mass transfer to the particle.

One way of presenting particle mass transfer between gas phase and solid particle is presented at Eq. 20. and 21. The reaction rate coefficient, k_i , is connected to the concentration of the surface of a particle, $Y_{i,s}$. It has to be noted that the reaction rate coefficient has to be presented at function of volume.

$$\begin{pmatrix} Particle & Mass \\ change \end{pmatrix} = \begin{pmatrix} Diffusion & to \\ surface \end{pmatrix} = \begin{pmatrix} Reaction & rate \\ inside & particle \end{pmatrix}$$
(20)

$$\pm \frac{dm_p}{dt} = h_m f_i S_p (Y_i - Y_{i,s}) = k_i V_p Y_{i,s}$$
(21)

Material	Fe	Cu	Ni
Reactivity properties with O2			
Reaction heat, J/kg	14749178,09	9754303,286	14981874,32
ρ_m , mol/m ³	22472	140251	151520
n	1,0	1,0	0,2
L, m	2,6 x 10 ⁻⁷	$2,3 \ge 10^{-10}$	5,8 x 10 ⁻⁷
k0	3,1 x 10 ⁻⁴	4,7 x 10 ⁻⁶	1,8 x 10 ⁻³
E, J/mol	1,4 x 10 ⁴	$1,5 \ge 10^4$	7,0 x 10^3
b	4	2	2
q	0,84	0,68	0,46
$ au_m$	4,71	3,43	24,4
Reactivity properties with CH4			
Reaction heat, J/kg	-2212957,986	2781854,32	-2445716,714
ρ_m , mol/m ³	$3,28 \ge 10^4$	8,04 x 10 ⁴	8,93 x 10 ⁴
n	1,3	0,4	0,8
L, m	2,6 x 10 ⁻⁷	4,0 x 10 ⁻¹⁰	6,9 x 10 ⁻⁷
k0	8,0 x 10 ⁻⁴	$4,5 \ge 10^{-4}$	7,1 x 10 ⁻¹
E, J/mol	4,9 x 10 ⁴	6,0 x 10 ⁴	7,8 x 10 ⁴
b	12	4	4
q	0	0	0
$ au_m$	0,889	0,0179	0,0217
Reactivity properties with CO			
Reaction heat, J/kg	-2936735,128	7931609,935	-2704038,901
ρ_m , mol/m ³	$3,28 \times 10^4$	8,04 x 10 ⁴	8,93 x 10 ⁴
n	1	0,8	0,8
L, m	2,6 x 10 ⁻⁷	4,0 x 10 ⁻¹⁰	6,9 x 10 ⁻⁷
k0	$6,2 \ge 10^{-4}$	5,9 x 10 ⁻⁶	$5,2 \ge 10^{-3}$
E, J/mol	2,0 x 10 ⁴	1,4 x 10 ⁴	2,5 x 10 ⁴
b	3	1	1
q	0,89	0,83	0,93
$ au_m$	4,59	5,45	11,18
Reactivity properties with H2			
Reaction heat, J/kg	-365451,204	5360388,515	-132817,481
ρ_m , mol/m ³	$3,28 \times 10^4$	8,04 x 10 ⁴	8,93 x 10 ⁴
n	0,8	0,6	0,5
L, m	$2,6 \ge 10^{-7}$	$4,0 \ge 10^{-10}$	6,9 x 10 ⁻⁷
k0	$2,3 \times 10^{-3}$	1,0 x 10 ⁻⁴	9,3 x 10 ⁻³
E, J/mol	2,4 x 10 ⁴	3,3 x 10 ⁴	2,6 x 10 ⁴
b	3	1	1
q	1,03	0,53	0,47
τ_m	1,24	0,322	6,62

 Table 5. Oxygen carrier reactivity properties

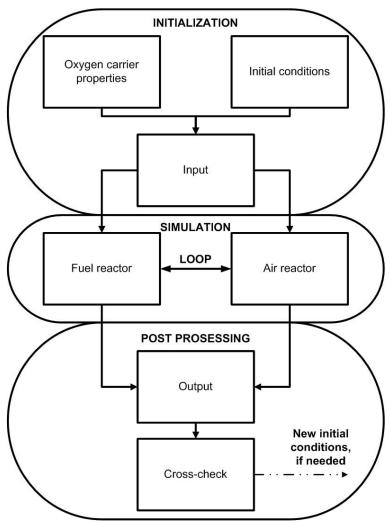


Figure 20. Model structure and simulation phases

where	h_m	is the mass transfer coefficient
	f_i	is the stoichiometric mass ratio
	S_p	is the particle surface area
	k_i	is the reaction rate coefficient
	Y_i	is the mass fraction of species i
	$Y_{i,s}$	is the mass fraction of species i at surface
	V_p	is the volume of particle

Another way of presenting mass transfer is the shrinking core model. Shrinking core model describes the effect of reaction and internal diffusion at Eq. 22.

$$\frac{dX_*}{dt} = \frac{1}{\frac{\tau_C}{3}(1 - X_*)^{-2/3} + 2\tau_D(1 - X_*)^{-1/3}}$$
(22)

where
$$X_*$$
is the conversion τ_C is the time for complete conversion under control of
diffusion τ_D is the time for complete conversion under control of
kinetics

Conversion and particle mass are connected which leads to equation, Eq. 23., where the reaction rate coefficient can be solved.

$$\pm \frac{dm_p}{dt} = \frac{S_p Y_i}{\frac{1}{f_i h_m} + \frac{(S_p / V_p)}{k_i(X)}}$$
(23)

The reaction rate coefficient, k_i , is usually obtained by an experimental relation. The reaction rate coefficient is calculated iteratively from measurements. A model to present reaction rate coefficient varies depending reaction and process. Model uses experimental relation, Eq. 24.

$$k_i(X_c) = k_{i^*}(X_c)Y_i^{n-1}$$
(24)

where X_c depends on reactor. At air reactor X_c is presented as X and at fuel reactor (1-X).

In this case, n is 1, which simplifies the equation. Notice that Eq. 24 may also depend on particle size.

Conversion, X, is defined from oxidation. Conversion is one when particle is fully oxidated and zero when particle is fully reduced. From definition Eq. 25. is deduced by mass and density change,

$$X = \frac{m_p - m_{p,min}}{m_{p,max} - m_{p,min}} = \frac{\rho_p - \rho_{min}}{\rho_{max} - \rho_{min}}$$
(25)

where	X	is the conversion
	m_p	is the mass of particle
	$m_{p,min}$	is the minimum mass of particle
	$m_{p,max}$	is the maximum mass of particle
	$ ho_p$	is the density of particle
	$ ho_{p,min}$	is the minimum density of particle
	$ ho_{p,max}$	is the maximum density of particle.

Particle mass, m_p , is calculated

$$m_p = \frac{\rho_p \pi d_p^3}{6} \tag{26}$$

where d_p is the particle diameter.

When earlier Eq. 22., 25. and 26. are deduced, the equation for the particle mass during oxidation can be presented as Eq. 27. Notice that particle shape is assumed to be spherical.

$$\pm \frac{dX}{dt} = \frac{(6/d)\frac{Y_i}{\Delta\rho_{max}}}{\frac{1}{f_i h_m} + \frac{(6/d_p)}{k_i(X)}}$$
(27)

where Y_i is the mass fraction $\Delta \rho_{max}$ is the maximum density change during oxidation and reduction

Surface area of a single particle, S_p , is calculated at Eq. 28.

$$S_p = \pi d_p^2 \tag{28}$$

S''', surface area of particle/volume of reaction, at Eq. 38 is presented at Eq. 29. Assumption is that particle is spherical.

$$S''' = (6/d)(1 - \varepsilon_b) \tag{29}$$

where	S'''	is particle surface area/volume of reactor
	ε_b	is the voidage of bed

Mass transfer of solid phase is solved at time steps. Particle motion and residence time are dependent on the reactor. These affect the gas phase because parts of the gas phase are solved as function of place. Particle motion is presented at Eq. 30. Notice that particle is assumed to be spherical and mono-sized.

$$m_p \frac{dw_p}{dt} = \frac{1}{2} A_p \rho_g C_d \left| w_g - w_p \right| (w_g - w_p) - m_p g \tag{30}$$

where	w_p	is the particle velocity
	w_g	is the gas velocity
	A_p	is the area of particle
	C_d	is the drag coefficient factor

Eq. 30 gives relationship between time and location.

Mass transfer of the gas phase can be calculated from change of solid mass function of time or mass flux as function of place. Mass change of gas phase is calculated by mass flux as function. This is easier because gas flow has been assumed to be plug flow. The mass exchange between gas and solid phase is presented at Eq. 31.

$$\frac{d\dot{m}_g}{dx} = \sum_i \frac{d\dot{m}_i}{dx} = (1-\epsilon)\frac{A}{V_p}\frac{dm_p}{dt} = -\frac{d\dot{m}_p}{dx}$$
(31)

Eq. 31. is simple, all mass which is increased to solid is taken from gas phase and vise versa. Eq. 32 is for a single species mass flux change presented as function of x. Remark that particle is assumed to be spherical.

$$\frac{d\dot{m}_i}{dx} = \frac{(AS'''Y_i)}{1/h_m + (6/d)/k_i(X)}$$
(32)

Mass flux change can be presented as Eq. 33, because there is only one reactant gas which interacts at each reactor. This simplifies the idea of how dependencies between phases are treated. Notice the assumptions that particle does not release mass to gas phase without reaction and reactions do not take place at the gas phase.

$$-\frac{d\dot{m}_g}{dx} = -\frac{d\dot{m}_i}{dx} = \pm \frac{d\dot{m}_p}{dx}$$
(33)

Depending on reaction, mass of particle will either decrease or increase.

3.4 Heat transfer

The energy equation for particle model is presented at Eq. 35. ΔH_i is the reaction heat, value is dependent on the reaction. Radiation heat transfer coefficient, h_r between reaction wall and particles are calculated from Eq. 36. Notice that particle temperature is assumed to be isothermal because of low temperature derivation at particle, as mentioned earlier at 2.3.3.

$$\begin{pmatrix} \text{Heat at} \\ \text{particle} \end{pmatrix} = \begin{pmatrix} \text{Convection} \end{pmatrix} + \begin{pmatrix} \text{Radiation} \end{pmatrix} + \begin{pmatrix} \text{Heat from} \\ \text{reaction} \end{pmatrix}$$
(34)

$$c_p m_p \frac{dT_p}{dt} = h_c S_p (T_g - T_p) + S_p h_r (T_w - T_p) + \Delta H_i \frac{dm_p}{dt}$$
(35)

where

c_p	is the specific heat capacity of particle
h_c	is the heat transfer coefficient at convection
h_r	is the heat transfer coefficient at radiation
T_{g}	is the temperature of gas
T_p	is the temperature of particle
T_w	is the temperature of wall
ΔH_i	is the reaction heat

$$h_r = F\varepsilon\sigma(T_w^2 + T_p^2)(T_w + T_p)$$
(36)

where	F	is the radiation coefficient
	ε	is the emissivity of particle
	σ	is the Stefan-Bolzmann's constant

The energy equation for gas phase is presented at Eq. 38. Note that equation is differentiated with respect to location, x, at reactor. Notice that the model is 1-

66

dimensional.

$$\begin{pmatrix} \text{Heat change of gas} \\ \text{depending location} \end{pmatrix} = \begin{pmatrix} \text{Heat from} \\ \text{particle} \end{pmatrix} + \begin{pmatrix} \text{Heat loss from} \\ \text{reactor} \end{pmatrix}$$
(37)

$$c_g \dot{m}_g \frac{dT_g}{dx} = h_c A_b S'''(T_p - T_g) + \phi'_c$$
(38)

where	c_g	is the specific heat capacity of gas
	$\dot{m_g}$	is the mass flow of gas
	A_b	is the cross area of bed
	ϕ_c'	is the heat loss from reactor

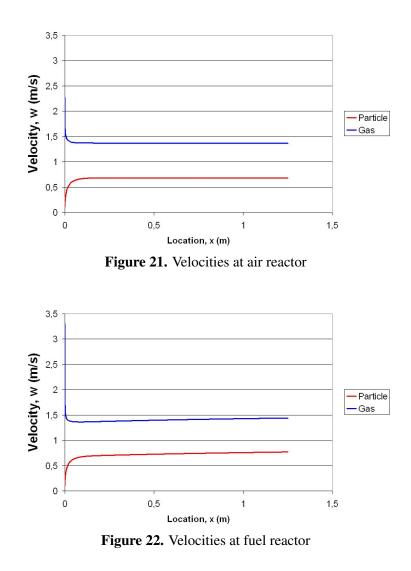
3.5 Results of model

The model gives output to table. Output contains a collection of main values and graphs from the simulation. The output values of the flows are essential when it comes to making a decision of whether the reactor design is suitable or not. The graphs provide more accurate information on how the reaction and process advance and what kind of differences there are between reactors.

Fig. 21. presents how velocities at air reactor develop. Particles are first at bubbling phase and the bed is quite dense until the particle velocity increases and rhe particle is entrained to gas flow.

Difference between reactors can be seen at Fig. 21. and 22. Fuel reactor reaction increases the amount of gas flow and velocities increase consequently.

Gas mass fraction change at fuel reaction can be seen at Fig. 23. for CH4 and H_2O . When combustion takes place CH4 decreases and H_2O increases. CO_2 is not presented at Fig. 23. because the scale of mass fraction is not same.



Conversion of fuel is important in order to create a feasible process. The conversion of fuel can be seen at Fig. 24. The conversion is presented as percentages to time. The flat part of the graph at the end presents the time where particle and gas are separated and reaction has stopped.

The conversion state of the oxygen carrier is important, especially with Fe-based oxygen carriers. Fig. 25. shows how the oxygen carrier conversion differs during location. If the conversion decreases low enough, the next oxidation cycle may be very slow.

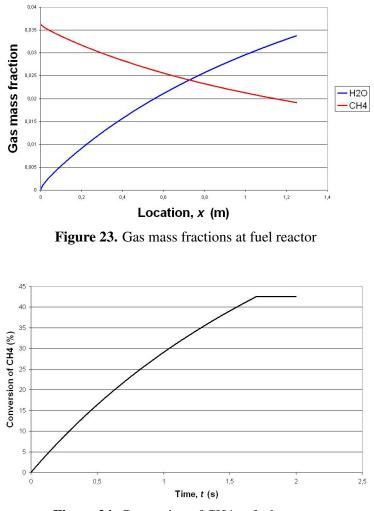


Figure 24. Conversion of CH4 at fuel reactor

If measured data is available, the data can be easily imported to graphs or graph data exported to other post-processing software. The accuracy of the graph is enough but the quality of the simulation cannot be reliably verified without any measured data. It is possible that the simulation provides too optimistic results due to reaction handling, numerical inaccuracies or model simplifications.

Results can be exported from the model depending on time or location. Also provisional results of the model can be presented as graph when needed. These results include temperatures, gas mass flow, voidage of bed, molar weight and density of the gas.

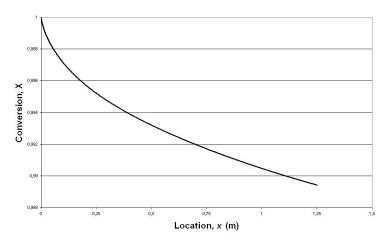


Figure 25. Conversion state of oxygen carrier at fuel reactor

4 REACTOR DESIGN

Desired features and properties need to be defined before the modeling and sizing of the reactor system. The purpose of this reactor system is to enable flexible testing of oxygen carriers. Physical properties and some design parameters can be seen at Table 6.

Reactor design for this kind of a system is not a simple process because oxygen carriers have a large variety of properties. Density, particle size and oxygen carrier capacity properties affect fluidization. Especially density and size change have a big effect on gas and particle velocities.

The reactor system should enable multiple kinds of research. Tests which should be possible to be performed with the constructed system are related to:

- oxygen carrier reactivity
- estimating kinetic parameters of an oxygen carrier
- long term durability of an oxygen carrier
- oxygen carrier mixtures
- gas leakage between reactors
- pressure distribution in reactor system
- validation of models
- scale-up verification
- recycling flue gas
- controlling the process/particle flow via double loop seal
- solid fuels at small scale

The reactor system has fixed properties and initial conditions which were given or decided. These properties and conditions are presented at Fig. 26. Figure is variation from Fig. 12. with additional arrow.

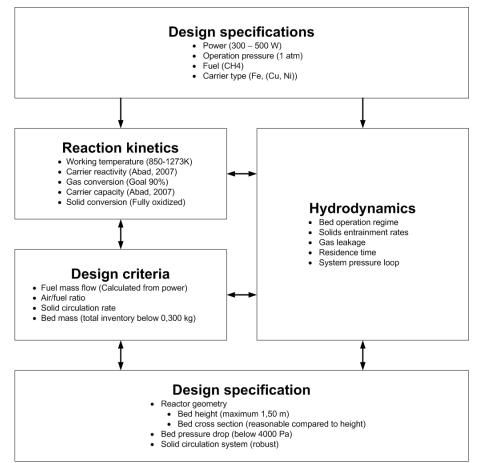


Figure 26. Design procedure with fixed properties and initial conditions

Because of the multitude of limiting conditions for the reactor system, the design interrelationship of variables became complicated. The model itself does include optimization of design parameters. Parameter runs are used to help sizing and selections. Interrelationships of main design and sizing variables are presented at Fig. 27.

4.1 Concept

The aim is to make possible the long term testing of oxygen carriers. Circulating continuous reactor design is essential for easy long term testing. This is why continuous reactor system was chosen as the concept. This is arranged by two circulation fluidized reactors with suitable particle locks and cyclones for solid-gas separation.

Limiting conditions have to be defined. One essential boundary is the desired thermal power. Thermal power is usually defined as W_{th} , which means the thermal

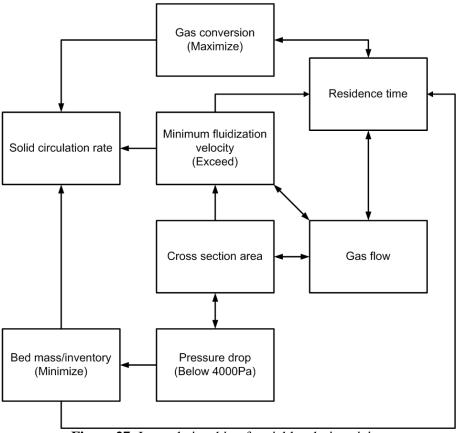


Figure 27. Interrelationship of variables during sizing

power of burned fuel. $300-500 \text{ W}_{th}$ was chosen as the thermal power range of the fuel reactor. This should be obtained with a Fe-based oxygen carrier.

Fuel gas feed is calculated from desired thermal power of 300 W_{th} , which is 6,0 mg/s CH₄ when thermal power of CH₄ is 50 MW_{th}/kg. Fuel gas flow itself is not high enough for needed fluidization. Needed gas velocity can be obtained by using CO₂ or N₂ as a driving gas.

Oxygen carrier circulation is defined from the fuel gas flow. Air excess was first determined as 1,2 for sizing. Minimum conversion of fuel gas should be 0,9 after fuel reactor. After the simulations, it was discovered that air excess cannot be used but particle mass flow is increased and gas flow decreased until the wanted fuel conversion and minimum fluidizing levels are obtained.

In literature, Fe-based oxygen carriers are considered as the weakest oxygen carriers. Ni- and Cu-based oxygen carriers should work well in the system because of their better reactivity. It has to be noted that reaction rate also differs between oxidation and reduction reactions.

	Air reactor	Fuel reactor
Height, m	1,4	1,25
Diameter, m	0,025	0,02
Cross section area, m ²	0,00049	0,000314
Working temperature, K	850-1273	850-1273
Flow direction	Upwards	Upwards
Design parameters		
Wall temperature, K	1173	1173
Conductance, W/mK	43	43
Effective radiation factor	0,3	0,3

Table 6. Physical properties of reactors

Particle size for sizing was taken from known oxygen carrier, which was 0,075–0,2 mm. Most influenced calculations were made with small diameters. Calculations are made with various diameters to be sure that system operates properly.

Rough and simple calculations and estimations from literature survey illustrate that solid inventory at whole system should be between 200–600 grams.

4.2 Reactor system

The concept of the reactor system is that it is divided into two reactors which are connected trough cyclones and particle locks. Both reactors have external heating with adjustable temperature. Reactors are divided into two separate furnaces. Both reactors are circulating fluidized bed reactors. The reactor concepts do not differ from each other.

In addition to the two reactors, reactor system includes cyclones, particle locks, loops and measurement devices. Every major part of the reactor system will be presented in the following sections.

4.2.1 Fuel reactor

Gas inlet is a mixed flow of CH_4 and CO_2 . Ratio difference of mixture changes depending on the oxygen carrier and the thermal power wanted. It is also possible

	Fe	Cu	Ni
Particle mass flow, kg/s	0,065	0,010	0,025
Gas mass flow, kg/s	0,000200	0,000150	0,000200
CH4/CO2 ratio at inlet	0,030/0,97	0,040/0,96	0,030/0,97
Burning efficiency, %	30,56	94,40	81,43
Minimum gas velocity, m/s	1,59	1,16	1,54
Residence time, s	1,31	1,392	1,30
Pressure drop, Pa	2663	434	1011
Inventory, kg	0,085	0,013	0,032

Table 7. Design properties of fuel reactor, particle diameter $200 \mu m$

to introduce nitrogen to the fuel reactor.

The reactor diameter is 0,02 meter, which means that the flow cross section area is $0,000314 \text{ m}^2$. Height of the air reactor is 1,25 m. The reactor diameter height ratio is 62,5. There is a plate at the bottom of the reactor which has a hole for the oxygen carrier and ash removal.

Sizing has been made with Fe -based oxygen carrier. After this, the suitability for Ni- and Cu -based oxygen carriers is tested. The properties and main result values from the model are presented in Table 7.

Particle mass flow, gas mass flow and fuel ratio differ because the densities and reactivity of oxygen carrier vary. Particle mass ow is selected to be high enough for good burner efficiency or low enough for reasonable mass ow. There is a visible difference between the oxygen carriers. Because Fe -based oxygen carrier has a relatively low reactivity, even a high amount of oxygen carrier will not provide wanted results. Temperatures at simulations have always been same (1173 K).

Particle mass flow, gas mass flow and fuel ratio differs, because densities and reactivity of oxygen carrier varies. Particle mass flow is selected to be high enough for good burner efficiency or low enough for reasonable mass flow. Difference can be seen between oxygen carriers. Because Fe -based oxygen carrier has relatively low reactivity, even high amount of oxygen carrier does not give wanted results. Temperatures at simulations have been same 1173 K.

Models with different oxygen carriers are not fully comparable but they do confirm that the same physical reactor is capable of using multiple different oxygen carriers. Reason for low inventory of Cu is low residence time, density of particle, large surface area and high reactivity.

Conversions of fuel for different oxygen carriers can be seen at Fig. 28. Models are made with same physical reactor design. Simulations have differences at gas and particle velocities and fuel composition.

Parameter runs for fuel reactor were made. Particle diameters of $75\mu m$ and $100\mu m$ were used in order to see how smaller particles react and behave. Graphs of parameter run are presented at Fig. 29. Conversion is highly dependent on particle mass flow and maximum particle velocity. This supports the concept of process because larger mass of the oxygen carrier and longer residence time increase conversion.

It would be best for the process if the particle size distribution would be narrow. Then the velocity could be adjusted according to the distribution used. For bigger particles, for example $200\mu m$, gas mass flow should be a lot higher. Note that the gas mass flow is the same in both cases.

4.2.2 Air reactor

It is easier to size an air reactor than a fuel reactor. An oxidation reaction is usually more faster than a reduction reaction. Gas is usually air. Sometimes syngas is used for testing. The air reactor is simulated with air, with oxygen-nitrogen ratio 0,231/0,769. The reacting gas is cheap and easy to obtain. Higher mass fraction of the reacting gas increases the reaction rate of oxidation compared to reduction.

The air reactor is usually designed as a driving reactor which has higher velocity and pressure. This will increase performance of the whole reactor system. The reactor diameter is 0,025 m, which means that the flow cross section area is 0,000490 m2. Height of the air reactor is 1,4 m. There is a plate at the bottom of the reactor which has a hole for oxygen carrier removal.

The reactor is a bit larger than a fuel reactor. When the diameter is higher, a higher volume ow can be used to force circulation. The air reactor is sized so that full conversion of oxygen carrier could be achieved. The properties and main result values from the model are presented in Table 8.

The key limiting conditions for the air reactor derive from Cu -based oxygen carrier.

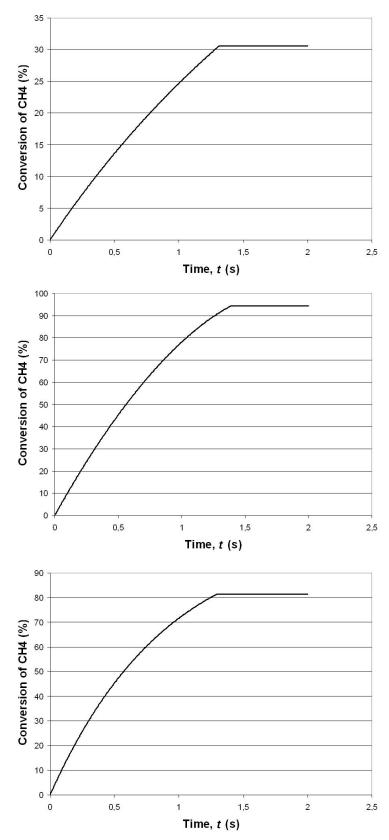


Figure 28. Conversion of fuel at fuel reactor, Fe-, Cu- and Ni-based oxygen carrier, particle diameter $200 \mu m$

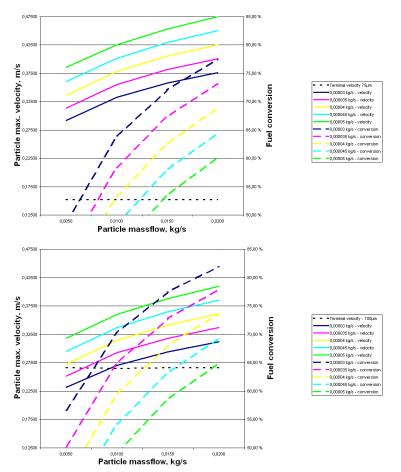


Figure 29. Parameter run of Fe-based oxygen carrier at fuel reactor with different gas mass flow, particle diameter $75 \mu m$ and $100 \mu m$

Table 8. Design	n properties of air reactor	r, particle diameter $200 \mu m$
-----------------	-----------------------------	----------------------------------

	Fe	Cu	Ni
Particle mass flow, kg/s	0,065	0,01	0,025
Gas mass flow, kg/s	0,0004	0,000175	0,00026
Minimum gas velocity, m/s	2,71	1,06	1,66
Residence time, s	0,744	2,02	1,44
Pressure drop, Pa	966	401	719
Inventory, kg	0,048	0,020	0,036

A small amount of Cu is used to burn fuel, about 20 % of oxygen carrier is reduced. This results in high conversion at the oxygen carrier, which requires a longer residence time. From Fig. 30. can been seen variation of conversion of the Cu -based oxygen carrier during oxidation and reduction reaction.

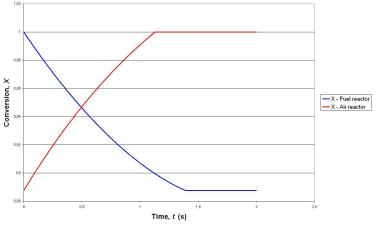


Figure 30. Conversion of Cu-based oxygen carrier

4.2.3 Cyclone

The reactor system has two cyclones. The cyclones are situated after the reactors and are sized after simulation because the gas inlet to the cyclone is dependent on the gas inlet to the reactor. It is not possible to use an additional fan after the reactor. This makes the sizing even more challenging.

Inlet speed to cyclone should be between 15.24–27.43 meters per second (Licht 1980). Because the volume flows are quite low at end of the cyclones, the inlet speed stays pretty low. The size of the cyclones can be decreased to increase inlet speed but this would increase pressure drop. As a compromise, sizing is done so that it is between adequately high inlet speed and reasonable pressure drop.

Cyclone shape and dimensions can be seen at Fig. 31. and Table 9.

Because volume flows are same scale at both reactors, same size cyclones can be used after both reactors.

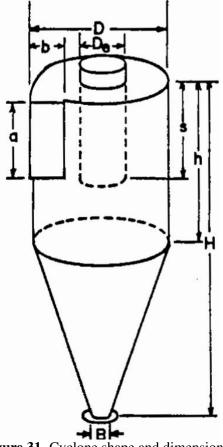


Figure 31. Cyclone shape and dimensions

4.2.4 Particle locks

There are two options for particle locks. First option is to use a basic elbow joint which is fluidized Fig. 32. Implementation to process is quite easy and control for fluidization is simple.

Another option is to use a loop-seal which has a double joint, Fig. 33. This option has at least two advantages. First, it is possible to use the loop-seal as a divider. One stream is to be recycled to the previous reactor and another stream is carried on to the next reactor. The second advantage is that a bigger particle mass flux can be reached. Sizing for particle locks has not yet been made. Note that at CLC process, fluidization gas is not air like it is shown in the picture.

Table 9.	Cyclone	dimen	sions
----------	---------	-------	-------

	Symbol	Fuel reactor	Air reactor
Height of inlet, mm	a	20	20
Width of inlet, mm	b	10	10
Diameter, mm	D	40	40
Cylinder height, mm	h	80	80
Diameter of vortex finder, mm	D_e	20	20
Height of vortex finder, mm	S	25	25
Total height, mm	Н	160	160
Diameter of collecting hopper, mm	В	10	10

4.2.5 Loops

Double exit particle loops make it possible to create loops to the reactor system. These loops are presented at Fig. 34. The figure shows the loops as a dotted line.

Recirculation is controlled via fluidization gas. Both sides of the double joint have gas inlet which can be controlled separately. If the gas flow from the recycle side of the loop is shut down, the joint works as a normal elbow joint.

4.3 Measurement

The reactor system is planned for testing different kinds of oxygen carriers at various conditions. It is important that the measurements are made at correct points at the system. The most important measurements are pressure, temperature and gas composition at outlet. Measurement locations can be seen at Fig. 34.

Pressure differences provide indirect information about the flow and circulation of the oxygen carrier. The measurements are located so that the pressure difference for the most essential process devices can be calculated. This may give information on the reason for a possible gas leakage. Manometers work at range of 0–5000 Pa.

Temperature is measured in order to control the process and heat exchange during use. Temperature measurements give information on how much heat is transferred to the fuel reactor from the air reactor by an oxygen carrier. Temperature measurements work at range of 0–1500 K.

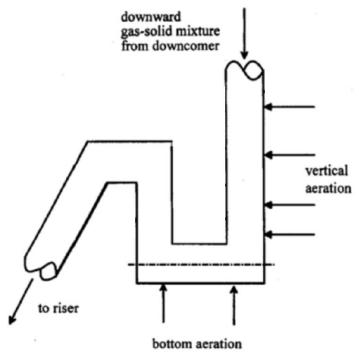


Figure 32. Schematic diagram of loop-seal (Kim et al. 1999)

On-line gas analysis is made from reactor outlets. O_2 , CO_2 , CH_4 need to be measured from the reactor's outlet. According to these measurements, it can be calculated how well the conversion has happened. The measurements also provide information on a possible gas leakage which may have taken place between the reactors. On-line gas analysis has to be calibrated with and without heat before the actual measurements. An outlet, including a simple valve, coming from the middle of the reactor and joint to the on-line analyzer is planned to increase knowledge and accuracy of parameter estimation. This will interrupt measurements from the normal outlet of the reactor, which is why it is used as an impulse measurement point.

In addition to this, we have flowmeters for inlets which are needed in order to get information on how much gas is introduced to the system. An inlet for gas is also added in front of the on-line analyzer because there may be situations where the outlet gas has to be diluted. Dilution may increase accuracy of measurement in such cases where gas flow is not high enough for the analyzer.

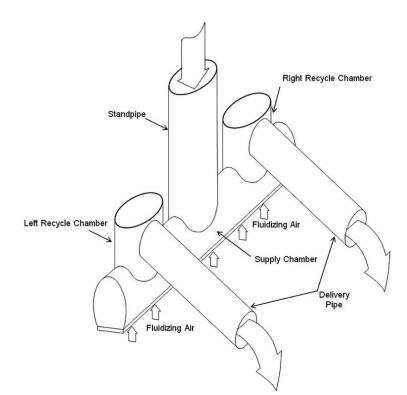


Figure 33. Loop-seal of a large commercial CFB boiler with a twin recycle chamber (Basu et al. 2009)

4.4 Conditions

The reactor system will be used in various conditions. The reactor system is at atmospheric pressure. Local pressure differences can occur but the differences are not significant for the reactor system. Temperature of the process may vary between 20-1350K. Depending on the oxygen carrier, the maximum temperature will be much lower than maximum.

The conditions are not corrosive for the reactor system. There are no statements about corrosion in literature. However, the inner side of the air reactor may oxidate during use. In the inner side of the fuel reactor, carbon from metal may burn during test, which may decrease the durability of the reactor.

Solid circulation makes it possible for some erosion to happen at the reactor system. The most vulnerable places for this kind of action are the cyclones and the bottom parts of the reactors. This is because most of the particle to wall interaction takes place there.

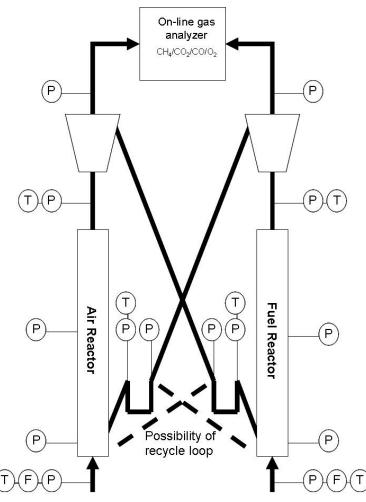


Figure 34. Locations for measurements at reactor design, P pressure, T temperature, F flowmeter

4.5 **Possible problems**

Most of the problems are connected to inefficient solid circulation. Key elements to prevent inefficient circulation are particle locks and suitable gas velocities. It is also possible that all oxygen carriers are not reactive enough for the desired fuel conversion.

4.5.1 Gas leakage between reactors

Gas leakage between emissions can decrease the efficiency of carbon capture. Pressure measurements and on-line analyses are the main tools for defining whether gas-leakage is happening and why. According to literature, there are a couple of main guidelines

Pressure in the fuel reactor should be higher than in the cyclone. The air reactor has to have higher pressure than the fuel reactor. Gas leakage is dependent on the particle velocity in the downcomer. If the particle velocity is too high, fluidization does not happen correctly and particle flow carries gas flow with it. (Johansson et al. 2003)

Typical value for gas leakage from cyclone is 2%. The leakage from air reactor to fuel reactor can vary between 2-12%. This dilutes carbon stream to carbon capture. This leakage can be decreased if steam is used for fluidization at loopseals. Johansson et al. (2003) mentions that even then gas leakage is not a major problem in the CLC design.

One way to investigate gas leakage is to input inert gas to the system during process and measure the concentrations from the on-line analyzer. For example helium is used for this.

4.5.2 Emissions

Emissions are not a big problem of CLC. Leakage from fuel reactor to air reactor releases carbon dioxide to the environment. Also a small amount of oxygen carriers may be lost during use.

 NO_x should not be formed during process. Only carbon dioxide may be released but at this scale, it would only decrease the efficiency of carbon capture. More severe harm from that would not occur.

4.6 Safety

Reactor system has to be safe to use. The reactor system is covered with furnaces, which prevents direct contact with the reactor system. Despite this, the reactor system and its surroundings will be hot and have to be insulated correctly. A cover for the reactor system also prevents problems if unwanted leakage of gas or solids would happen.

When in normal use, the pressure at the reactor system is not high or low enough to produce problems. Misuse or malfunction may change the pressure, but it should easily be below the reactor's maximum pressure resistance level.

Important moments from the point of view of safety are start up and shutdown. Start up and shutdown have to be completed controllably and smooth. This is possible with the help of good automation.

Start up has to be done slowly, especially when the reactor system is used for the first time, because the system has never been heated before. The heating has to be done with solid circulation because then the heat gets more evenly distributed. Uneven distribution of heat may cause tensions and stress to junctions. If the heating is not done slowly, the seams and junctions may leak. It is also important to secure the junctions after use.

Shutdown should be done with sliding control. Heat from furnaces can be decreased and fuel gas can be changed to nitrogen. This way, the reactions will stop. After this, the heating can be shut down. Depending on what kind of research is done, oxygen carrier can be exported from the reactor system while it is still hot, or the reactor system may be cooled down first. It is essential that it is cooled down safely if the oxygen carrier is exported at high temperature.

Automated shutdown sequence has to be done in case of malfunction or incident. This has to be tested before any actual research tests. Unnecessary immediacy to the reactor system while testing should be avoided because of heat and the possibility of malfunction.

4.6.1 Toxicity

Some of the oxygen carriers are toxic. For example nickel compounds are usually toxic and can cause e.g. lung cancer. It is important to prevent nickel compounds from getting into lungs. This has to be made sure when oxygen carriers are inserted or taken out of the reactor system. Also leakages may expose user to the oxygen carrier.

If the reactor system has a gas leakage outside the system, it is possible that the gas may be hazardous to human health. Gas leakage from an air reactor is not as

risky as leakage from a fuel reactor. Leakage from an air reactor may decrease the oxygen level near the leakage location.

Leakage from a fuel reactor may contain more hazardous gases. CO_2 and CO levels near the leakage point can raise very fast. Also, if the leakage occurs near the fuel junction, it is possible that the leakage gas is highly flammable.

4.7 Design summary

The design can be divided into two parts: its physical properties and variable properties. At first, the diameter for the reactor was 0,05 meters, but it was found to be too large for the desired inventory. The reactor diameter was then decreased, which produced higher conversion, smaller gas mass flow and inventory. The smaller size of the diameter also made it possible to use higher fuel ratio at gas feed, which increased conversion.

Diameter below 0,02 meters may decrease circulation ability and increase pressure drop. Also, hot spots at reactor may occur if the diameter is too narrow, but this possibility is not confirmed. As a conclusion, the diameter for the fuel reactor was chosen to be 0,025 meters. For the air reactor, the suitable diameter may be larger because the reaction takes place faster and the goal is just to produce fully oxidized particles and robust circulation.

Suitable conversion with low enough inventories were obtained with the height of 1,20 meters at the fuel reactor and 1,40 meter for the air reactor. The air reactor could be shorter, but to insure full conversion, a higher reactor was chosen. The placement of the reactor system does not allow room for a system higher than 1,50 meters. Higher reactors also increase the costs of the system.

Variable properties include the mass of inventory, velocities and residence time. After the physical properties are selected, these depend on the oxygen carrier. Because particle diameter and density affect to terminal velocity, these properties vary depending on the oxygen carrier. The physical design was made mainly for Fe -based oxygen carrier. Suitability for other oxygen carriers was tested after that.

Note that the velocities presented at Table 10. are for Fe -based particles of $200\mu m$ diameter. Particle diameter for sizing was chosen to be bigger than normally be-

REACTOR	Symbol	Air	Fuel
Height, m	H _{reac}	1,40	1,25
Diameter, m	D _{reac}	0,025	0,020
Working temperature, K		850-1273	850-1273
Inventory, g		75–150	75–150
Pressure drop, Pa		1000-3500	1000-4000
Average gas velocity, Fe, m/s		2,71	1,63
Minimum gas velocity, m/s		2,72	1,58
Residence time, s		0,5-2,5	1,312
CYCLONE	Symbol	Air	Fuel
Height of inlet, mm	a	20	20
Diameter, mm	D	40	40
Cylinder height, mm	h	80	80
Diameter of vortex finder, mm	D_e	20	20
Height of cone, mm	h_c	80	80
Total height, mm	Н	160	160
Inlet velocity, m/s		1–2	1–2
Pressure drop, Pa		2000–2500	2000-2500

Table 10. Main reactor system dimensions and area of operation, symbol refers to Fig. 35.

cause the reactor should work for a variety of particles. Smaller particle diameter would decrease velocities and increase conversion.

Fig. 35. is not in scale.

Velocities, inventories and residence times, which are used at future cannot be estimated, but reactor design works for large scale of velocities and inventories. Probably is that most of oxygen carrier can be tested at the reactor system when inventory and gas flow velocities are adjusted to be suitable for used oxygen carrier.

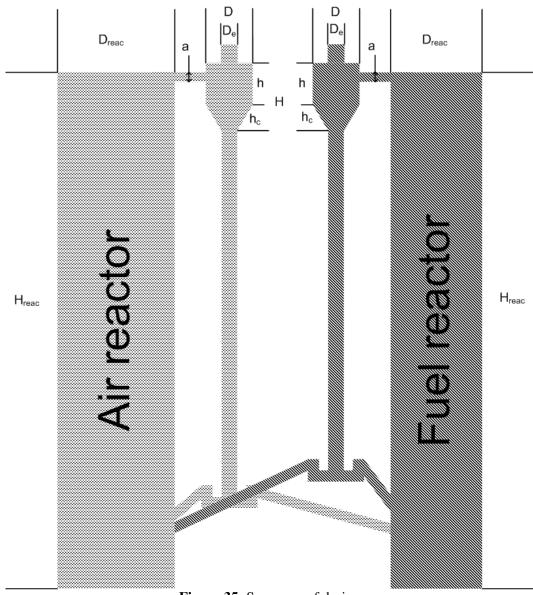


Figure 35. Summary of design

5 RESULTS AND DISCUSSION

This thesis consists of a profound literature survey in the field of chemical looping combustion. Chemical looping combustion has proven its potential as an energy efficient way to decrease carbon dioxide emissions. In this thesis, multiple different reactor and process designs have been reviewed and both their advantages and disadvantages have been discussed.

For this paper, a particular concept and reactor system has been designed and sized. The reactor system consists from an air and a fuel reactor and supporting equipments for process. The air reactor height is 1,40 meters and diameter 0,025 meters. The fuel reactor height is 1,20 meters and diameter is 0,02 meters.

From the perspective of concept designing, it was quite easy to view different kinds of concepts and look for the best selections and exclude the worst. A more challenging task was to combine the good selections and good designs into one.

The aim of the reactor system design was to provide a system which has a well working circulation with multiple different oxygen carriers at two different reactors. In the future, measurements have to be designed to support the surveys. The designed reactor system is well balanced for different kinds of surveys.

The reactor system was designed and sized. Finding reasonable reactivity and fuel conversion level proved to be the most difficult part. The reason for this was the lack of reactivity of Fe -based oxygen carrier. No major difficulties were to be found with other oxygen carriers during modeling and sizing.

Decencies between particle properties and hydrodynamic were challenging because of the variety of the particles. Multiple simulation runs were made and the suitability for various particles and fluid velocities was obtained.

A mathematical model was used to model conversion and major variables at reactors. A preliminary model was made for the air reactor. The upgraded model is now compatible with both the fuel reactor and reduction reaction. During development, a few changes were also made to the model for the air reactor. The model is now versatile to be estimated in future surveys.

Major improvements for the model and simulation were made to improve the us-

ability and suitability for reactor sizing. The theory behind the mathematical model itself has been left untouched.

5.1 Future work

Lots of work has to be done before the surveys. If the cold model tests, which probably already have been done, support the calculations of this thesis, a fully working reactor system will be constructed as it has been designed.

A functioning reactor system provides the possibility to test different oxygen carriers in a versatile manner. The reactor system can be used to do tests for suitable amount of inventory, different kinds of fuel combustion, pressure losses with different inventory and different mathematical model verification. Also gas leakage tests and measurements for reactivity properties estimation can be done.

When more measurement data is available, applied model can be updated to be more accurate for the oxygen carrier used. This will increase scalability to bigger combustion system. During this thesis, raw measurement data for modeling and reactor design was not available. Data and properties for simulations are taken from literature and an exact way of testing the procedure is not known. This has to be taken into account when evaluating the design and sizing. Here, mere assumptions had to be sometimes made but additional measurement data and the possibility to perform tests with the reactor system will fill some of the gaps.

Chemical looping combustion research is going to increase around the world. There are some main fields which research probably will emphasize more.

One of these interesting fields of research is the burning of solid fuels with chemical looping combustion. If solid fuels can be used at chemical looping combustion, it probably will be included to coal combustion. This is important also when biomass combustion is studied. CLC combined to biomass combustion would bind carbon dioxide from the atmosphere.

There are several 3D models of the combustion process. The overall development of modeling is heading this way. 1D models are used for sizing and quick simplified analyses but because computational capacity and new techniques develop all the time, more complicated models will be used. These models may not be more accurate at first but in the long run, information provided by these models will increase.

REFERENCES

- Abad, A., Adánez, J., Garcia-Labiano, F., de Diego, L. F. & Gayán, P. (2009), 'Modeling of the chemical-looping combustion of methane using a cu-based oxygencarrier', *Combustion and Flame* **157**(3), 602 – 615.
- Abad, A., Adánez, J., Garcia-Labiano, F., de Diego, L. F., Gayán, P. & Celaya, J. (2007), 'Mapping of the range of operational conditions for cu-, fe-, and ni-based oxygen carriers in chemical-looping combustion', *Chemical Engineering Science* 62(1-2), 533 549. Fluidized Bed Applications.
- Abad, A., Adánez, J., Garcìa-Labiano, F., de Diego, L. F., Gayán, P. & Pröll, P.
 K. T. (2010), Clc modeling: the fuel-reactor at fast fluidization conversion of ch4 using a nio-based oxygen-carrier in a 120 kwth unit, *in* 'Les Rencontres Scientifiques de l'IFP 1st International Conference on Chemical Looping'.
- Abad, A., Mattisson, T., Lyngfelt, A. & Rydén, M. (2006), 'Chemical-looping combustion in a 300 w continuously operating reactor system using a manganesebased oxygen carrier', *Fuel* 85(9), 1174 – 1185.
- Abdulally, I., Andrus, H., Thibeault, P. & Chiu, J. (2010), Alstom?s chemical looping combustion coal power technology development prototype, *in* 'Les Rencontres Scientifiques de l'IFP - 1st International Conference on Chemical Looping'.
- Adánez, J., de Diego, L. F., García-Labiano, F., Gayán, P., Abad, A. & Palacios, J. M. (2004), 'Selection of oxygen carriers for chemical-looping combustion', *Energy & Fuels* 18(2), 371–377.
- Adánez, J., Dueso, C., de Diego, L. F., García-Labiano, F., Gayán, P. & Abad, A. (2009), 'Methane combustion in a 500 wth chemical-looping combustion system using an impregnated ni-based oxygen carrier', *Energy & Fuels* 23(1), 130–142.
- Adánez, J., García-Labiano, F., de Diego, L. F., Gayán, P., Celaya, J. & Abad, A. (2006), 'Nickel-copper oxygen carriers to reach zero co and h2 emissions in chemical-looping combustion', *Industrial & Engineering Chemistry Research* 45(8), 2617–2625. author = Adánez, Juan and García-Labiano, Francisco and de Diego, Luis F. and Gayán, Pilar and Celaya, Javier and Abad, Alberto,.
- Adánez, J., Gayán, P., Celaya, J., de Diego, L. F., García-Labiano, F. & Abad, A. (2006), 'Chemical looping combustion in a 10 kwth prototype using a cuo/al2o3 oxygen carrier: Effect of operating conditions on methane combustion', *Industrial & Engineering Chemistry Research* 45(17), 6075–6080.

- Balaji, S., Ilic, J., Ydstie, B. E. & Krogh, B. H. (2010), 'Control-based modeling and simulation of the chemical-looping combustion process', *Industrial & Engineering Chemistry Research* **49**(10), 4566–4575.
- Basu, P. & Butler, J. (2009), 'Studies on the operation of loop-seal in circulating fluidized bed boilers', *Applied Energy* **86**(9), 1723–1731.
- Basu, P., Chandel, M., Butler, J. & Dutta, A. (2009), 'An investigation into the operation of the twin-exit loop-seal of a circulating fluidized bed boiler in a thermal power plant and its design implication', *Journal of Energy Resources Technology* 131(4), 041401.
- Basu, P. & Cheng, L. (2000), 'An analysis of loop seal operations in a circulating fluidized bed', *Chemical Engineering Research and Design* **78**(7), 991–998.
- Beal, C., Vandycke, M. & Andrus, H. E. J. (2009), Alstom chemical looping technology advancement, *in* '1st International Oxy-Combustion Conference'.
- Bolhàr-Nordenkampf, J., Pröll, T., Kolbitsch, P. & Hofbauer, H. (2009), 'Comprehensive modeling tool for chemical looping based processes', *Chemical Engineering & Technology* 32(3), 410–417.
- Cao, Y., Casenas, B. & Pan, W.-P. (2006), 'Investigation of chemical looping combustion by solid fuels. 2. redox reaction kinetics and product characterization with coal, biomass, and solid waste as solid fuels and cuo as an oxygen carrier', *Energy & Fuels* 20(5), 1845–1854.
- Chong, Y.-O., Nicklin, D. & Tait, P. (1986), 'Solids exchange between adjacent fluid beds without gas mixing', *Powder Technology* **47**(2), 151–156.
- Cloete, S., Johansen, S. T. & Amini, S. (2010), Multiphase cfd-based models for a chemical looping combustion process, *in* 'Les Rencontres Scientifiques de l'IFP 1st International Conference on Chemical Looping'.
- de Diego, L. F., García-Labiano, F., Adánez, J., Gayán, P., Abad, A., Corbella, B. M. & María Palacios, J. (2004), 'Development of cu-based oxygen carriers for chemical-looping combustion', *Fuel* 83(13), 1749–1757.
- Deng, Z., Xiao, R., Jin, B. & Song, Q. (2009), 'Numerical simulation of chemical looping combustion process with caso4 oxygen carrier', *International Journal of Greenhouse Gas Control* 3(4), 368–375.

- Fang, H., Haibin, L. & Zengli, Z. (2009), 'Advancements in development of chemical-looping combustion: A review', *International Journal of Chemical En*gineering 2009, 1–16.
- Fang, M., Yu, C., Shi, Z., Wang, Q., Luo, Z. & Cen, K. (2003), 'Experimental research on solid circulation in a twin fluidized bed system', *Chemical Engineering Journal* 94(3), 171–178.
- Garcìa-Labiano, F., de Diego, L. F., Adánez, J., Abad, A. & Gayán, P. (2005), 'Temperature variations in the oxygen carrier particles during their reduction and oxidation in a chemical-looping combustion system', *Chemical Engineering Science* **60**(3), 851 – 862.
- Håkonsen, S. F., Dahl, I. M., Stange, M., Spjelkavik, A. I. & Blom, R. (2010), On the development of a rotating reactor concept for chemical looping combustion part 2, *in* 'Les Rencontres Scientifiques de l'IFP 1st International Conference on Chemical Looping'.
- Hossain, M. M. & de Lasa, H. I. (2008), 'Chemical-looping combustion (clc) for inherent co2 separations–a review', *Chemical Engineering Science* 63(18), 4433 – 4451.
- Ishida, M. & Jin, H. (1994), 'A novel combustor based on chemical-looping reactions and its reaction kinetics', *Journal of chemical engineering of Japan* 27(3), 296–301.
- Ishida, M. & Jin, H. (1996), 'A novel chemical-looping combustor without nox formation', *Industrial & Engineering Chemistry Research* **35**(7), 2469–2472.
- Jerndal, E., Mattisson, T. & Lyngfelt, A. (2006), 'Thermal analysis of chemicallooping combustion', *Chemical Engineering Research and Design* 84(9), 795 – 806. Carbon Capture and Storage.
- Jerndal, E., Mattisson, T., Thijs, I., Snijkers, F. & Lyngfelt, A. (2009), 'Nio particles with ca and mg based additives produced by spray- drying as oxygen carriers for chemical-looping combustion', *Energy Procedia* **1**(1), 479–486.
- Jerndal, E., Mattisson, T., Thijs, I., Snijkers, F. & Lyngfelt, A. (2010), 'Investigation of nio/nial2o4 oxygen carriers for chemical-looping combustion produced by spray-drying', *International Journal of Greenhouse Gas Control* **4**(1), 23–35.
- Johansson, E., Lyngfelt, A., Mattisson, T. & Johnsson, F. (2003), 'Gas leakage measurements in a cold model of an interconnected fluidized bed for chemicallooping combustion', *Powder Technology* **134**(3), 210–217.

- Johansson, M. (2007), Screening of oxygen-carrier particles based on iron-, manganese-, copper- and nickel oxides for use in chemical-looping technologies, PhD thesis, Chalmers University of Technology.
- Johnsson, F., Andersson, S. & Leckner, B. (1991), 'Expansion of a freely bubbling fluidized bed', *Powder Technology* **68**(2), 117–123.
- Jung, J. & Gamwo, I. K. (2008), 'Multiphase cfd-based models for chemical looping combustion process: Fuel reactor modeling', *Powder Technology* 183(3), 401– 409.
- Kim, S., Namkung, W. & Kim, S. (1999), 'Solids flow characteristics in loop-seal of a circulating fluidized bed', *Korean Journal of Chemical Engineering* 16, 82–88. 10.1007/BF02699009.
- Kolbitsch, P., Bolhàr-Nordenkampf, J., Pröll, T. & Hofbauer, H. (2010), 'Operating experience with chemical looping combustion in a 120 kw dual circulating fluidized bed (dcfb) unit', *International Journal of Greenhouse Gas Control* 4(2), 180 185. The Ninth International Conference on Greenhouse Gas Control Technologies.
- Kolbitsch, P., Pröll, T., Bolhar-Nordenkampf, J. & Hofbauer, H. (2009), 'Design of a chemical looping combustor using a dual circulating fluidized bed (dcfb) reactor system', *Chemical Engineering & Technology* **32**(3), 398–403.
- Kolbitsch, P., Pröll, T. & Hofbauer, H. (2009), 'Modeling of a 120 kw chemical looping combustion reactor system using a ni-based oxygen carrier', *Chemical Engineering Science* 64(1), 99 – 108.
- Kronberger, B., Johansson, E., Löffler, G., Mattisson, T., Lyngfelt, A. & Hofbauer, H. (2004), 'A two-compartment fluidized bed reactor for co2 capture by chemical-looping combustion', *Chemical Engineering & Technology* 27(12), 1318–1326.
- Kruggel-Emden, H., Rickelt, S., Stepanek, F. & Munjiza, A. (2010), 'Development and testing of an interconnected multiphase cfd-model for chemical looping combustion', *Chemical Engineering Science* In Press, Corrected Proof, –.
- Kunii, D. & Levenspiel, O. (1977), *Fluidization engineering*, Robert E. Krieger Publishing Company, Inc.
- Leion, H., Jerndal, E., Steenari, B.-M., Hermansson, S., Israelsson, M., Jansson, E., Johnsson, M., Thunberg, R., Vadenbo, A., Mattisson, T. & Lyngfelt, A. (2009),

'Solid fuels in chemical-looping combustion using oxide scale and unprocessed iron ore as oxygen carriers', *Fuel* 88(10), 1945 – 1954.

- Leion, H., Mattisson, T. & Lyngfelt, A. (2007), 'The use of petroleum coke as fuel in chemical-looping combustion', *Fuel* **86**(12-13), 1947 1958.
- Leion, H., Mattisson, T. & Lyngfelt, A. (2008), 'Solid fuels in chemical-looping combustion', *International Journal of Greenhouse Gas Control* **2**(2), 180 193.
- Licht, W. (1980), Air pollution control engineering: basic calculations for particulate collection, Pollution engineering and technology, M. Dekker.
- Linderholm, C., Abad, A., Mattisson, T. & Lyngfelt, A. (2008), '160 h of chemical-looping combustion in a 10-kw reactor system with a nio-based oxygen carrier', *International Journal of Greenhouse Gas Control* 2(4), 520 530. TCCS-4: The 4th Trondheim Conference on CO2 Capture, Transport and Storage.
- Linderholm, C., Jerndal, E., Mattisson, T. & Lyngfelt, A. (2010), 'Investigation of nio-based mixed oxides in a 300-w chemical-looping combustor', *Chemical Engineering Research and Design* 88(5-6), 661–672.
- Linderholm, C., Mattisson, T. & Lyngfelt, A. (2009), 'Long-term integrity testing of spray-dried particles in a 10-kw chemical-looping combustor using natural gas as fuel', *Fuel* 88(11), 2083–2096.
- Lyngfelt, A. (2010), Oxygen-carriers for chemical-looping combustion operational experience, *in* 'Les Rencontres Scientifiques de l'IFP - 1st International Conference on Chemical Looping'.
- Lyngfelt, A., Johansson, M. & Mattisson, T. (2008), Chemical-looping combustion - status of development, *in* '9th International Conference on Circulating Fluidized Beds (CFB-9)'.
- Lyngfelt, A., Kronberger, B., Adanez, J., Morin, J.-X. & Hurst, P. (2004), The grace project. development of oxygen carrier particles for chemical-looping combustion. design and operation of a 10 kw chemical-looping combustor., *in* '7th International Conference on Greenhouse Gas Control Technologies'.
- Lyngfelt, A., Leckner, B. & Mattisson, T. (2001), 'A fluidized-bed combustion process with inherent co2 separation; application of chemical-looping combustion', *Chemical Engineering Science* 56(10), 3101 – 3113.

- Lyngfelt, A. & Thunman, H. (2005), Construction and 100 h of operational experience of a 10-kw chemical-looping combustor, *in* 'Carbon Dioxide Capture for Storage in Deep Geologic Formations', Elsevier Science, Amsterdam, pp. 625– 645.
- Pröll, T., Kolbitsch, P., Bolhàr-Nordenkampf, J. & Hofbauer, H. (2010), Operation of a chemical looping pilot plant up to 150 kw fuel power - results for a nickel-based oxygen carrier and discussion of further scale-up scenarios, *in* 'Les Rencontres Scientifiques de l'IFP - 1st International Conference on Chemical Looping'.
- Pröll, T., Rupanovits, K., Kolbitsch, P., Bolhàr-Nordenkampf, J. & Hofbauer, H. (2009), 'Cold flow model study on a dual circulating fluidized bed (dcfb) system for chemical looping processes', *Chemical Engineering & Technology* 32(3), 418–424.
- Raiko, R., Kurki-Suonio, I., Saastamoinen, J. & Hupa, M. e. (2002), *Poltto ja palaminen*, International Flame Research Foundation Suomen kansallinen osasto.
- Richter, H. & Knoche, K. (1983), 'Reversibility of combustion processes, in efficiency and costing - second law analysis of processes.', ACS symposium series. pp. 71–85.
- Riehle, C. (2000), 'Measuring and calculating solid carry over in a cfb cold flow model for different materials', *Powder Technology* **107**(3), 207–211.
- Rydén, M., Cleverstam, E., Lyngfelt, A. & Mattisson, T. (2009), 'Waste products from the steel industry with nio as additive as oxygen carrier for chemical-looping combustion', *International Journal of Greenhouse Gas Control* **3**(6), 693–703.
- Rydén, M., Lyngfelt, A. & Mattisson, T. (2008), 'Chemical-looping combustion and chemical-looping reforming in a circulating fluidized-bed reactor using ni-based oxygen carriers', *Energy & Fuels* 22(4), 2585–2597.
- Ryu, H.-J., Jin, G.-T. & Yi, C.-K. (2004), Demonstraion of inherent co2 separation and nox emission in a 50kw chemical-looping combustor: Continuous reduction and oxidation experiment, *in* 'Proceedings of the 7th International Conference on Greenhouse Gas Control Technologies'.
- Ryu, H.-J., Park, Y.-C., Jo, S.-H. & Park, M.-H. (2008), 'Development of novel twointerconnected fluidized bed system', *Korean Journal of Chemical Engineering* 25(5), 1178–1183.

Saastamoinen, J. (2010), 'Conversation and personal written notes', Unpublished.

- Snijkers, F., Jerndal, E., Thijs, I., Mattisson, T. & Lyngfelt, A. (2010), Preparation of oxygen carriers for chemical looping combustion by industrial spray drying method, *in* 'Les Rencontres Scientifiques de l'IFP - 1st International Conference on Chemical Looping'.
- Son, S. R. & Kim, S. D. (2006), 'Chemical-looping combustion with nio and fe2o3 in a thermobalance and circulating fluidized bed reactor with double loops', *Industrial & Engineering Chemistry Research* 45(8), 2689–2696.
- Tallón, C., Yates, M., Moreno, R. & Nieto, M. I. (2007), 'Porosity of freeze-dried [gamma]-al2o3 powders', *Ceramics International* 33(7), 1165–1169.
- Xu, M., Ellis, N., Lim, C. J. & Ryu, H.-J. (2009), Mapping of the operating conditions for an interconnected fluidized bed reactor for co2 separation by chemical looping combustion, *in* 'Chemical Engineering & Technology', pp. 404–409.
- Zafar, Q., Mattisson, T. & Gevert, B. (2006), 'Redox investigation of some oxides of transition-state metals ni, cu, fe, and mn supported on sio2 and mgal2o4', *Energy & Fuels* 20(1), 34–44.